https://ntrs.nasa.gov/search.jsp?R=19750020850 2020-03-22T19:52:51+00:00Z

General Disclaimer

One or more of the Following Statements may affect this Document

- This document has been reproduced from the best copy furnished by the organizational source. It is being released in the interest of making available as much information as possible.

- This document may contain data, which exceeds the sheet parameters. It was furnished in this condition by the organizational source and is the best copy available.

- This document may contain tone-on-tone or color graphs, charts and/or pictures, which have been reproduced in black and white.

- This document is paginated as submitted by the original source.

- Portions of this document are not fully legible due to the historical nature of some of the material. However, it is the best reproduction available from the original submission.

Produced by the NASA Center for Aerospace Information (CASI)

X-602-75-163
PREPRINT

NASA TM X- 70935

HYBRID THEORY AND CALCULATION OF $e\text{-}N_2$ SCATTERING

(NASA-TM-X-70935) HYBRID THEORY AND CALCULATION OF e-N2 SCATTERING (NASA) 54 p HC $4.25 CSCL 20L
N75-28923
Unclas
G3/76 29834

N. CHANDRA
A. TEMKIN

AUG 1975
RECEIVED
NASA STI FACILITY
INPUT BRANCH

JUNE 1975

GSFC
GODDARD SPACE FLIGHT CENTER
GREENBELT, MARYLAND

HYBRID THEORY AND CALCULATION OF $e-N_2$ SCATTERING

N. Chandra* and A. Temkin
Theoretical Studies Group, Goddard Space Flight Center,
National Aeronautics and Space Administration,
Greenbelt, Maryland 20771

ABSTRACT

A theory of electron-molecule scattering is developed which is a synthesis of close coupling and adiabatic-nuclei theories. Specifically the theory is close coupling with respect to vibrational degrees of freedom but adiabatic-nuclei with respect to rotation. In addition, this theory can be applied to any number of partial waves required, the remaining ones can be calculated purely in one or the other approximation. A theoretical criterion based on fixed-nuclei calculations and not on experiment can be given as to which partial waves and energy domains require the various approximations. The theory allows all cross sections (i.e., pure rotational, vibrational, simultaneous vibration-rotation, differential and total) to be calculated. Explicit formulae for all these cross sections are given.

*NRC-NASA Resident Research Associate.

The theory is applied to low energy e-N_2 scattering. The fixed-nuclei results are such that the criterion shows clearly that vibrational close coupling is necessary, but only for the $^1\Pi_g$ partial wave. The contribution of remaining partial waves can be obtained directly from the adiabatic-nuclei approximation. The close coupling calculation for the $^1\Pi_g$ wave is carried out, and we find that it does give rise to the substructure as well as the gross structure of the 2.4 eV resonance. When this amplitude is combined with the adiabatic amplitudes we can compute absolute values of all cross sections of interest. In particular we find that vibrational excitation cross sections are about twice as large as previously inferred. The momentum transfer cross section can also be computed, and it too reveals substructure within the gross structure resonance.

I. INTRODUCTION

Molecular nitrogen is a major constituent of the atmosphere to an altitude of about 500 km. Thus it can be expected that the scattering of electrons from N_2 will be an important process in the aeronomy of the atmosphere particularly above the E region, where photoionization of many of the upper atmospheric constituents by solar UV produces an abundance of electrons. For example the resonances in the e-N_2 vibrational excitation cross sections in the vicinity of 2.4 eV have been used by Newton et al.,[1] to explain an enhanced $O^+ + N_2(v) \rightarrow NO^+ + N$ rate which in turn will lead to the observed decrease in ambient electron density in the F_2 region during times of enhanced air-glow giving rise to stable auroral red (SAR) arcs via the reaction $e + NO^+ \rightarrow N + O$.

The 2.4 eV, e-N_2 resonance is known to be a very complex structure. Fortunately there is a wealth of experimental details,[2] and more or less phenomonological theories to explain them. It is important however that this complicated structure be understood from a fundamental—essentially ab initio point of view, inorder that researchers be able to predict scattering from other molecules which cannot be prepared in the laboratory, but which we now know to exist in many astrophysical environments.[3] We believe that the present modification and synthesis of existing theories will complete the fundamental approximations which must underlie the methodologies to be employed in such calculations.

In Section II we shall describe the e-N_2, 2.4 eV resonance and briefly review the previous calculational theories leading to the point in Section III that strictly on the basis of fixed-nuclei calculations (and not experiment) of the Π_g partial wave, one can infer that the adiabatic-nuclei theory will not suffice to describe the substructure of the resonance.[4] The fixed-nuclei calculations which are an extension of those of Burke and Chandra[5] to a series of internuclear distances R are also described in Section III. In Section IV we develop the vibrational-close coupling theory and show that our calculations for the Π_g partial wave do reveal the substructures of this resonance as more states are added while at the same time showing reasonable convergence when a sufficient number of states is retained. The main formulae of the adiabatic-nuclei approximation are reviewed in Section V; by simple inspection one may then see how to combine the vibrational close coupling with adiabatic-nuclei theories: the process is one of substitution of the appropriate scattering matrices of the one theory for the corresponding ones of the other.

Results and comparisons with experiment are also given in Section V. An important aspect of the calculations is that they yield absolute normalization for individual vibrational excitation cross sections, whereas as far as we know all measurements are relative or have been done at individual angles. Furthermore the theory is complete: it gives formulae for total and differential cross sections of individual and averaged transitions for vibrational and or rotational

excitation as well as pure elastic scattering. Simultaneous vibration, rotation differential cross sections can also be calculated (although that is not done here) as well as the momentum-transfer. The latter, which is calculated, is particularly interesting because it reveals substructure similar to that of the elastic scattering.

Finally in Section VI we give a brief discussion of how this method fits in with other methods and possible generalizations.

II. PRELIMINARIES

Experimentally the low energy $e-N_2$ resonance is a complicated beast. It was first measured in detail in vibrational excitation by Schulz[6] as a series of irregular peaks (cf. Figs. 11, 12 & 13). The results have been importantly complemented by the measurement of the vibrationally elastic scattering by Golden,[7] which shows a gross structure peak centered at about 2.4 eV superimposed on top of at least five prominent sub peaks between 1.8 and 3.2 eV (cf. Fig. 7). The observed inelastic structure of the led in short order to its interpretation (crudely described) as a compound state of the electron and target system i.e., the N_2^- ion)[8, 9] with the substructure due to the interference between the various vibrational states of the compound system. This general physical interpretation of the structure is certainly correct; the difficulty with the calculations is that they are not ab initio, and thus they contain many adjustable parameters. It should be added, however, that the physical and mathematical refinements of this general approach have been greatly developed since the original

papers, most successfully by Birtwistle and Herzenberg.[10] That calculation which is based on a boomerang model, gives remarkable agreement with the shapes of the vibrational excitation curves as measured by Ehrhardt and Willmann[11] but it too does not give absolute values.

In addition to the types of calculations mentioned above, there have been other, more ab initio types of investigations. One is a calculation by Krauss and Mies[12] of N_2^- as a bound state structure. This calculation confirmed the assignment by Gilmore[13] of this resonance as a Π_g "state," and it showed that it is a shape rather than a Feshbach resonance. The calculation is truly a 15 electron self-consistent field calculation, but since the Π_g symmetry overlaps the ordinary $e\text{-}N_2$ continuum, which can be of lower energy, some delicate restrictions on the variation were necessary to assure that the resonant state was not contaminated by this nonresonant scattering of the same symmetry. On that score we can all state that the calculation was in good hands with the NBS investigators.[12]

Finally two single-center fixed-nuclei calculations have been carried out by the Belfast group: the first by Burke and Sinfailam[14] includes full exchange of the incident and orbital electrons, but no induced polarization; the second by Burke and Chandra[5] includes polarization and simulates exchange by orthogonalizing the scattered to the bound orbitals. This 'pseudo-potential' approach provides the basis of all fixed-nuclei aspects of the present calculation, and we shall discuss it as appropriate in succeeding sections.

III. FIXED-NUCLEI THEORY AND CALCULATIONS

In contrast to its application in bound state problems, the fixed-nuclei approximation for electron-molecule scattering[15,16] assumes not only that the nuclei are fixed (at a distance R apart), but that the target molecular wave function $\Phi(x; R)$ has been precalculated at each, in principle arbitrary, internuclear separation R. As a result the scattering associated with a total wave function (r is the coordinate of the scattered and χ_i those of the orbital electrons)

$$\Psi_\ell^{(m)} = \psi_m(r; R)\, \Phi(x_i; R) \tag{3.1}$$

exhibits no particular stationary properties with respect to variations of R about the equilibrium separation of the target molecule $R = R_o$. This is a very forcefully exhibited here, when we extend the calculations at the equilibrium separation.[3] ($R = R_o = 2.068a_o$) to four additional values of R of the N_2 wave function given by Nesbet:[17] R = 1.744393, 1.868, 2.268, 2.391607.

To review the fixed-nuclei calculation (cf. Ref. 5 but our notation is somewhat different), the ground state $^1\Sigma_g^+$ of N_2 is a closed shell described by a single Slater determinant

$$\Phi = \det\left(\phi_{\alpha_1}(x_1)\, \phi_{\alpha_2}(x_2) \ldots \phi_{\alpha_{14}}(x_{14})\right) \tag{3.2}$$

where the α_i can readily identified from the configuration $1\sigma_g^2\ \ 2\sigma_g^2\ \ 3\sigma_g^2\ \ 1\sigma_u^2\ \ 2\sigma_u^2\ \ 1\pi_u^4$ of the ground, $^1\Sigma_g^+$, state of N_2. The bound state function[17] which is an LCAO function-meaning pairs of orbitals are centered about the separate nuclei—is converted to a single center basis using a program of Faisal and Tench.[18]

$$\phi_\alpha(r) = \sum_{\ell \geq \lambda_\alpha}'' \frac{1}{r} \phi_\ell^\alpha(r) Y_{\ell\lambda_\alpha}(\Omega) . \tag{3.3}$$

(A double prime indicates every second term is to be taken. About eight terms in this expansion are sufficient for convergence.) A similar expansion is now made of the scattered orbital[16]

$$\Psi_m(r) = \sum_{\ell}'' \frac{u^{(m)}_{\ell_i \ell_j}(r)}{r} Y_{\ell_i m}(\Omega) Y^*_{\ell_j m}(\Omega_o) , \tag{3.4}$$

where Ω_o are the sperical angles of the internuclear axis in the laboratory frame and $r = (r, \Omega)$, i.e., unprimed coordinates are the coordinates in the molecular frame.

With the use of (3.3) the static potential seen by the scattered electron is naturally expanded in single center coordinates (in rydberg units)

$$\left\langle \Phi \left| \frac{2Z}{|r - R/2|} + \frac{2Z}{|r + R/2|} - \sum_{i=1}^{N} \frac{2}{|r - r_i|} \right| \Phi \right\rangle = \sum_{\lambda}'' V_\lambda(r) P_\lambda(\cos\theta) \tag{3.5}$$

The equations satisfied are then derived from the variational principle:

$$\delta \int \Psi_\ell^{(m)*} (H - E) \Psi_\ell^{(m)} \, d\tau = 0 \tag{3.6a}$$

which is equivalent to the projection

$$\int Y^*_{\ell_i m} Y_{\ell_j m} (H - E) \Psi_\ell^{(m)} \, dr^{-1} = 0 \tag{3.6b}$$

where dr^{-1} means integration over all coordinates but r (including integration over Ω_o). In practice this set of coupled equations, which may readily be

derived from (3.1) - (3.5), is augmented to include an induced polarization potential

$$V^{(pol)}(r; R) = -\left(\frac{\alpha_0(R)}{r_>^4} + \frac{\alpha_2(R)}{r_>^4} P_2(\cos\theta)\right)[1 - e^{-(r/r_0)^6}], \qquad (3.7)$$

where $r_>$ is greater of r and ½R. The calculation[5] also includes orthogonality to all occupied orbitals of the same symmetry via Lagrange multipliers. The equations satisfied by $u_{\ell_i\ell_j m}(r)$ of Equation (3.4) are then

$$\left(\frac{d^2}{dr^2} - \frac{\ell_i(\ell_i+1)}{r^2} + k^2\right) u^{(m)}_{\ell_i\ell_i}(r) - \sum_j v^{(m)}_{\ell_i\ell_j}(r)\, u^{(m)}_{\ell_i\ell_j}(r) = \sum_\alpha \lambda_\alpha\, \phi^{(\alpha)}_{\ell_i}(r), \qquad (3.8)$$

where

$$v^{(m)}_{\ell_i\ell_j} = \sum \sqrt{\frac{2\ell_j - 1}{2\ell_i + 1}}\, (\ell_j\, \lambda\, o\; o/\ell_i\; o)(\ell_j\, \lambda\, m\; o/\ell_i\; m)\, v_\lambda(r), \qquad (3.9)$$

and

$$v_\lambda(r) = V_\lambda(r) + V^{(pol)}_\lambda(r). \qquad (3.10)$$

$V^{(pol)}_\lambda$ are the multiple components of V^{pol} from (3.7), thus in particular $V^{(pol)}_\lambda = 0$ for $\lambda > 2$. [The remaining symbols in (3.9) are Clebsch-Gordan coefficients.]

The calculation for each R was done just as the calculations of Burke and Chandra[5] at $R = R_0$. One only needs the dependence of the polarizabilities on R. These were taken of the form

$$\alpha_0(R) = 12.0 + 1.692(R - R_0) \qquad (3.11a)$$

$$\alpha_2(R) = 4.2 + 2.031(R - R_0) \qquad (3.11b)$$

Equations (3.11) were chosen to give the correct polarizabilities at $R = R_o$ and to reduce correctly to the united atom limit: $\alpha_0(0)$ $[= \alpha_{silicon}] = 8.5a_o^3$ and $\alpha_2(0) = 0$. The value $8.5a_o^3$ was interpolated from Sternheimer's[19] calculation of the polarizabilities of Cl^-, K^+, and Ca^{++}. It is to be noted that Equations (3.11) are somewhat different from Truhlar[20] who used Raman data to get an accurate estimate of the derivatives in the neighborhood of $R = R_o$. Our own interpolations, while somewhat cruder, should apply over a larger range in R, and thus be more suitable to excitation of higher lying vibrational states. Finally the value of r_o was retained at 1.592 as independent of R. That value was chosen,[5] so that the Π_g resonance for $R = R_o$ occured at exactly $k^2 = 2.394$ eV.

The scattering is determined from the asymptotic solution of (3.8):

$$\lim_{r\to\infty} u^{(m)}_{\ell_i\ell_j} = k^{1/2}\left\{\sin\left(kr - \frac{\pi\ell_i}{2}\right)\delta_{\ell_i\ell_j} + K^{(m)}_{\ell_i\ell_j}\cos\left(kr - \frac{\pi\ell_j}{2}\right)\right\} \tag{3.9}$$

The K matrix as indicated in (3.9) is diagonal in m; it is also real, symmetric, and for homonuclear targets connects only ℓ_i and ℓ_j of the same parity. In matrix notation the scattering is naturally expressed in terms of a matrix proportional to the T matrix. In Reference 5 this matrix is taken to be $T^{(m)}$ which is related to $K^{(m)}$ by

$$T^{(m)} = 2i(1 - iK^{(m)})^{-1} K^{(m)} \tag{3.10}$$

In Reference 16, which gives the original derivation of the coupled fixed nuclei cross sections (using a spherical analysis), the scattering is written in terms of the a matrix which is related to the above T matrix by[21]

$$a_{\ell_i \ell_j m} = i^{\ell_i - \ell_j - 1} \frac{\sqrt{\pi(2\ell_j + 1)}}{k} T^{(m)}_{\ell_i \ell_j} \tag{3.11}$$

The fixed-nuclei results are most conveniently given in terms of the sum eigenphase shifts. The eigenphases are the arc tangents of the eigenvalues of the K matrix:

$$\det |K^{(m)} - \lambda^{(m)} I| = 0 \tag{3.12a}$$

$$\Delta^{(m)} = \sum_i \tan^{-1} \lambda_i^{(m)}, \tag{3.12b}$$

where the sum in (3.12b) goes over all coupled states that are included (and is found to converge with inclusion of approximately 8 coupled states as stated above.) I is the unit matrix. In Table I we give a selection of our results for Σ_g, Σ_u, Π_u partial waves as a function of internuclear separation R. The $R(=R_o) = 2.068$ results are just those of Burke and Chandra.[5] A detailed description of that generic program has been published by one of us[22] and that program is what was applied here.

We also note in addition to m = 0, 1, ... corresponding to Σ, Π, ... that the parity of the index ℓ (even or odd corresponding to g or u) is also a good quantum number as well as the spin S. The latter is always S = ½ corresponding to doublet multiplicity, since N_2 is a closed shell ($^1\Sigma_g$) target. [We therefore suppress the doublet label, for example $^2\Pi_g$, on our partial wave notation.]

The sum of eigenphases for non-Π_g phase shifts are seen to change minimally as a function of R (although it is interesting that for Σ_g the minute change is

an oscillatory one). The change is also slow and smooth as function of the impacting energy k^2. For those partial waves therefore the adiabatic-nuclei theory for both rotational and vibrational excitation applies (see below).

On the other hand the change with both R and k^2 of the Π_g wave, given in Figure 1, is dramatic! As a function of k^2 the subient feature is the resonant behaviour. If one confines attention to the equilibrium separation R_e, one[5] evaluates the width $\Gamma \cong 0.4\,eV$, which is sensibly larger than the vibrational spacing $\Delta E_v \cong 0.29\,eV$. It was for this reason that we previously believed the adiabatic nuclei theory would be at least semi-quantitatively applicable to that partial wave as well.[23] However if one looks at the curves for $R > R_o$ then one sees that the resonance has diminished to $\Gamma \cong 0.14\,eV$ for $R = 2.391607$. And even at $R = 2.268$, $\Gamma \cong 0.25\,eV$ which is smaller than the vibrational spacing of N_2; in other words the time ($\tau \propto \Gamma^{-1}$) spent by the incoming electron in the vicinity of the molecule is comparable to or longer than the vibrational period of the nuclei. This is a definite violation of a basic criterion for the validity of the adiabatic-nuclei theory, and it gives a purely theoretically determined basis for distrusting the adiabatic-nuclei theory for this partial wave.[24] We therefore turn in the next section to vibrational close coupling and its amalgamation into the adiabatic-nuclei theory.

Before concluding this section, we give in Figure 2 a comparison of our fixed-nuclei width and position curves vs. R as compared to the calculations of

Krauss and Mies[12] and Birtwisth and Herzenberg.[10] Considering the different natures of these calculations, we consider the agreement to be remarkable.

IV. VIBRATIONAL CLOSE COUPLING

It is clear from the foregoing that it is necessary to include the dynamical response of the nuclei to their vibrational motion. The most natural way of doing that in quantum mechanics is to expand the wave function in terms of the eigenfunctions of the vibrational motion: this is what is meant by a vibrational close coupling expansion:

$$\Psi^{(m)} = \Phi(r_i; R) \sum_v F_v^{(m)}(r)\, \chi_v(R) \tag{4.1}$$

[The contrast of this with (3.1) should be noted.] Let us write the total Hamiltonian (in rydbergs)

$$H = H_0(R) - \nabla_r^2 - \frac{1}{M} \nabla_R^2 + V_{ee} + V_{Ne} \tag{4.2}$$

where $H_0(R)$ is the Hamiltonian the target molecule, with nuclei at a distance R apart and M their reduced mass. V_{ee} and V_{Ne} are the interaction potentials of the scattered electron with the orbital electrons and nuclei respectively:

$$V_{ee} = \sum_{i=1}^{N} \frac{2}{(r - r_i)} \tag{4.3}$$

$$V_{Ne} = -2Z\left(\frac{1}{|r - R/2|} + \frac{1}{|r + R/2|}\right) \tag{4.4}$$

We derive coupled equations for the functions $F_v(r)$ in the usual way; obtaining:

$$[-\nabla_r^2 - k_{v'}^2]\, F_{v'}(r) + \sum_v \langle \Phi v' | V_{ee} + V_{Ne} | \Phi v \rangle_{R, r_i} F_v(r) = 0 \tag{4.5}$$

In deriving (4.5) one uses the conservation of energy

$$E - E_o = k^2 + \epsilon_o = k_v^2 + \epsilon_v \tag{4.6}$$

where E_o is the electronic energy of the target state satisfying the target Schrodinger equation:

$$H_o(R)\, \Phi(r_i, R) = E_o(R)\, \Phi(r_i, R) \tag{4.7}$$

One also uses the approximation that the rotational kinetic energy is negligible compared to its vibrational energy, so that

$$\nabla_R^2 \to \frac{1}{R} \frac{d^2 R}{dR^2} \tag{4.8}$$

and the fact

$$\left[-\frac{1}{M} \frac{1}{R} \frac{d^2 R}{dR^2} + \langle \Phi(r_i, R) | H_o(R) | \Phi(r_i, R) \rangle_i - \epsilon_v \right] \chi_v(R) = 0 \tag{4.9}$$

In (4.5) and (4.9) the subscripts on $\langle\ \rangle$ indicate the coordinates over which one integrates. Note in particular that $\langle \Phi v' | V_{ee} | \Phi v \rangle_{R, r_i}$ includes the parametric dependence of Φ on R and is therefore not simply $\delta_{vv'} \langle \Phi | V_{ee} | \Phi \rangle_{r_i}$. On the other hand it is true that

$$\langle \Phi v' | V_{Ne} | \Phi v \rangle_{R, r_i} = \langle v' | V_{Ne} | v \rangle_R \tag{4.10}$$

since Φ is normalized for each R and V_{Ne} is independent of r_i. The net results is that the set of equations, (4.5) is seen to be a set of equations purely in r.

To eliminate the angular dependence we make the usual type spherical harmonic expansion. As opposed to (3.4), however, we here suppress the dependence on Ω_o, since this does not alter the dynamical equations. Let

$$F_{\nu}^{(m)}(\vec{r}) = \frac{1}{r} \sum_{\ell} f_{\nu\ell}^{(m)}(r) Y_{\ell m}(\Omega) \tag{4.11}$$

$$\langle \Phi \,|V_{ee} + V_{Ne}|\, \Phi \rangle_{r_i} = \sum_{\lambda} V^{(\lambda)}(r, R)\, P_{\lambda}(\cos\theta) \tag{4.12}$$

The latter implies that

$$\langle \Phi\nu' \,|V_{ee} + V_{Ne}|\, \Phi\nu \rangle_{R, r_i} = \sum_{\lambda} V_{\nu'\nu}^{(\lambda)}(r)\, P_{\lambda}(\cos\theta) \tag{4.13}$$

where

$$V_{\nu'\nu}^{(\lambda)}(r) = \langle \nu' \,|V^{(\lambda)}(r, R)|\, \nu \rangle_R \tag{4.14}$$

Using all these plus the well known formula for the integral of three spherical harmonics[25]

$$\int Y_{\ell' m}^{*} P_{\lambda}\, Y_{\ell m} d\Omega = (-1)^{m} [(2\ell' + 1)(2\ell' + 1)]^{1/2} \begin{pmatrix} \ell' & \lambda & \ell \\ m & o & -m \end{pmatrix} \begin{pmatrix} \ell' & \lambda & \ell \\ o & o & o \end{pmatrix} , \tag{4.15}$$

one can reduce (4.5) to the coupled equations:

$$\left[\frac{d^2}{dr^2} - \frac{\ell'(\ell' + 1)}{r^2} + \kappa_{\nu'}^2\right] f_{\nu'\ell'}^{(m)}(r) = \sum_{\nu, \ell, \lambda} \sqrt{(2\ell + 1)(2\ell' + 1)}\, (-1)^{m} \begin{pmatrix} \ell' & \lambda & \ell \\ m & o & -m \end{pmatrix} \begin{pmatrix} \ell' & \lambda & \ell \\ o & o & o \end{pmatrix} v_{\nu'\nu}^{(\lambda)}(r)\, f_{\nu\ell}^{(m)}(r) \tag{4.16}$$

Equation (4.16) shows that the price we have to pay to get rid of the angles in (4.5) is the ℓ coupling. In addition to that we have the summation over λ which comes from the single-center spherical expansions of V_{ee} and V_{Ne}, Equations (4.3), (4.4). Finally however in the spirit of our fixed-nuclei

calculation we include an additional pseudo-potential to describe and simulate the effects of polarization and exchange. [Note, like (3.1), (4.1) is also not anti-symmetrized between r and r_i (i = 1, 2, . . , N)]. However the way to do is now clear: to $V^{(\lambda)}_{v'v}(r)$ we add a polarization potential gotten from appropriate matrix elements of $V^{(pol)}$ (r, R) of (3.7). i.e., in (4.5) we augment the potential by $\langle \Phi v' | V^{pol} | \Phi v \rangle$; this induces a change in the potential $V^{(\lambda)}_{v'v}$ of (4.14) to $\Upsilon^{(\lambda)}_{v'v}(r)$ in Equation (4.16), where

$$\nu^{(\lambda)}_{v'v} = V^{(\lambda)}_{v'v}(r) + \langle v' | V^{(pol)}_{\lambda} | v \rangle_R \tag{4.17}$$

and $V^{(pol)}_{\lambda}$ is the λ^{th} multiple component of $V^{(pol)}$ [see below Equation (3.10)].

Equations (4.16) are solved in analogous fashion to (3.8) specifically here one demands the asymptotic form

$$\lim_{r \to \infty} f^{(m)}_{v'\ell'}(r) = \frac{1}{\sqrt{k_v}} \left\{ \sin\left(k_{v'} r - \frac{\pi \ell'}{2}\right) \delta_{vv'} \delta_{\ell\ell'} + K^{(m)}_{v'\ell', v\ell} \cos\left(k_v r - \frac{\pi \ell}{2}\right) \right\} \tag{4.18}$$

From the $K^{(m)}$ matrix one can, in analogy with (3.10) and (3.11), develop a $T^{(m)}$ and $\mathcal{A}^{(m)}_{v'\ell', v\ell}$ matrix

$$T^{(m)}_{v'\ell', v\ell} = 2i \sum_{v'', \ell''} (1 - i K^{(m)}_{v'\ell', v''\ell''})^{-1} K^{(m)}_{v''\ell'', v\ell} \tag{4.19}$$

$$\mathcal{A}^{(m)}_{v'\ell', v\ell} = i^{\ell' - \ell - 1} \frac{\sqrt{\pi(2\ell + 1)}}{k_v} T^{(m)}_{v'\ell', v\ell} \tag{4.20}$$

The actual calculation, as we have indicated, need only be done for the Π_g partial wave. For this partial wave there is no orthogonality requirement, on the other hand the multiplicity of coupling (v, ℓ, and λ) makes it impossible, even on our machine (IBM 360-91), to include a sufficient number of terms to get full convergence in all coupling indices. We have therefore chosen to delimit the ℓ coupling to three terms ($\ell = 2, 4, 6$). The λ expansion is thereby automatically restricted to seven terms ($\lambda = 0, 2, \ldots, 12$). Within this approximation we seek convergence in v. The role of the polarization potential $V^{(pol)}$, specifically the cut-off r_o here will serve, in addition to exchange, to simulate the unincluded ℓ and λ components. It was chosen so that with the inclusion of only one vibrational state, the resonance in the $v = 0 \rightarrow v = 0$ cross section occured at $k_o^2 = 2.4\,eV$ (cf. Fig. 4).

We shall not dwell on the numerical aspects of this calculation: suffice it to say that the generic program of Reference 22 was applicable with only minor additions to (4.16). The static potentials $V_{v'v}^{(\lambda)}(r)$ were generated numerically from Nesbet's wave functions;[17] a selection of these potentials as a function of r is shown in Figure 3. There diagonal potentials are compared with the fixed nuclei (static) potentials $V^{(\lambda)}(r, R_o)$ wherein we see that both potentials get increasingly more sharply peaked and concentrated around $r = R_o/2$, but that for corresponding λ the close coupling potentials are softer and without cusps. The off diagonal potentials have no real counterpart in the adiabatic-nuclei theory, and they are mathematically the source of the substructure of the Π_g resonance.

To see how this substructure appears we show in Figure 4 the Π_g contribution to the $v = 0 \rightarrow v' = 0$ cross section. The cross section is plotted for different numbers of vibrational states retained in the expansion. In addition we have shown two sets of curves, one includes two coupled $\ell(\ell = 2, 4)$ components in (4.16) and one set includes three ℓ's (2, 4, 6). For each case we include all λ allowed by vector coupling.

One can see that one v term result does indeed exhibit a resonance at $k^2 = 2.4\,eV$. It was essential to get this resonance that the polarization potential be included along with the static potential in $V^{(\lambda)}$. To get the resonance at the desired position we had to chose $r_o = 1.496$, 1.554 for two—and three ℓ-coupled calculations respectively. These values are gratifyingly close to the value needed in the fixed-nuclei calculation 1.597.[5] Thereafter one sees as the fundamental result of this paper that the substructure begins to appear, and that by the time we have coupled in 10 and 9 vibrational states respectively, reasonable (but not precision) convergence is seen to occur. (The program correctly includes whether various vibrational channels are energetically closed or open.)

The comparison of the two vs. three coupled ℓ solutions shows that detailed effects do depend on the number of ℓ's retained. Thus to obtain the second rather than the first bump as dominant in σ_{oo} as is revealed by experiment (cf. Fig. 13), the retention three ℓ's is necessary. It is also clear that the inclusion of even more ℓ's would be necessary to obtain the totality of peaks in the substructure.

(We shall see other manifestations of the truncated substructure in other cross sectioned data as well.)

In Figures 5 and 6 we give similar results for the (Π_g contribution) to $v = 0 \rightarrow 1$ and $v = 0 \rightarrow 2$ cross sections. The same type of convergence and ℓ-coupling effects are apparent, except that the necessity of more ℓ-coupling (and consequently more v coupling) becomes progressively greater, as one goes to higher v'.

We also state for the record that the substructure does not appear if we retain only one ℓ. Nor does it occur in the adiabatic-nuclei approximation[23] (see below).

V. ADIABATIC-NUCLEI APPROXIMATION, HYBRID THEORY, RESULTS

The adiabatic-nuclei approximation[26] gives the transition amplitude between vibrational, rotational states $\Gamma \rightarrow \Gamma'$ as

$$f_{\Gamma'\Gamma}(\xi,\Omega') = \langle \Gamma' | f(\xi, \Omega') | \Gamma \rangle_\xi + \epsilon \qquad (5.1)$$

where $f(\xi, \Omega')$ is the fixed-nuclei amplitude with nuclear coordinates frozen at ξ. Although the error term ϵ on the RHS of (5.1) has never been completely elucidated, the present calculation will show that the delay time of scattering must be small compared to the period $\tau \cong \hbar_i/\Delta E_{\Gamma'\Gamma}$ associated with the largest energy quantum number of Γ which changes in the transition (we assume $\Gamma' \neq \Gamma$), in order for ϵ to be neglibible. The fixed-nuclei amplitude for scattering from a diatomic molecule[6] is such the angular integrations in (4.1) can be done analytically,[27] whereas the integrations over R are necessarily numerical.

The resulting formula for the simultaneous rotation-vibration differential cross section (when the target is a Σ_g^+ state) can be written[28]

$$\frac{d\sigma_{j'v';jv}}{d\Omega'} = \frac{k_{j'v'}}{k_{jv}} \frac{1}{4\pi} \sum_L A_L(j'v'; jv)\, P_L(\cos\theta') \tag{5.2a}$$

where

$$A_L(j'v'; jv) = (2L+1)(2j'+1) \sum (-1)^{\ell_j + \lambda_j + m + \mu} \sqrt{(2\ell_i+1)(2\lambda_i+1)}\, a_{\ell_i \ell_j m}(v'v)$$

$$a^*_{\lambda_i \lambda_j \mu}(v'v) \begin{pmatrix} \ell_i & \lambda_i & L \\ o & o & o \end{pmatrix} \begin{pmatrix} \ell_j & \lambda_j & L \\ o & o & o \end{pmatrix} \sum_J (-1)^J \begin{pmatrix} \ell_i & \ell_j & J \\ m & -m & o \end{pmatrix} \begin{pmatrix} \lambda_i & \lambda_i & J \\ \mu & -\mu & o \end{pmatrix} \tag{5.2b}$$

$$\begin{pmatrix} j' & j & J \\ o & o & o \end{pmatrix}^2 \begin{Bmatrix} \ell_i & \lambda_i & L \\ \lambda_j & \ell_j & J \end{Bmatrix}$$

and for joint vibration-rotational excitation[29]

$$a_{\ell_i \ell_j m}(v', v) = \int_0^\infty \chi_{v'}(R)\, a_{\ell_i \ell_j m}(R)\, x_v(R)\, R^2\, dR \tag{5.3}$$

If one averages over initial rotational states j and sums over final states j', one arrives at

$$\frac{d\sigma_{v',v}}{d\Omega'} = \frac{k_{v'}}{k_v} \frac{1}{4\pi} \sum A_L(v', v)\, P_L(\cos\theta) \tag{5.4a}$$

where the rotationally averaged coefficients are:

$$A_L(v', v) = (2L+1) \sum [(2\ell_i+1)(2\lambda_i+1)]^{1/2}\, a_{\ell_i \ell_j m}(v', v)\, a^*_{\lambda_i \lambda_j \mu}(v', v) \tag{5.4b}$$

$$\begin{pmatrix} \ell_i & \lambda_i & L \\ o & o & o \end{pmatrix} \begin{pmatrix} \ell_j & \lambda_j & L \\ o & o & o \end{pmatrix} \begin{pmatrix} \ell_i & \lambda_i & L \\ m & \mu & -(m+\mu) \end{pmatrix} \begin{pmatrix} \ell_j & \lambda_j & L \\ m & \mu & -(m+\mu) \end{pmatrix} P_L(\cos\theta')$$

The total cross are quite obviously just 4π times the L = 0 terms of the respective expressions

$$\sigma_{j'v',jv} = \frac{k_{j'v'}}{k_{jv}} A_o(j'v'; jv) \tag{5.5}$$

$$\sigma_{v',v} = \frac{k_{v'}}{k_v} \sum \frac{1}{(2\lambda+1)} |a_{\ell\lambda m}(v'v)|^2 \tag{5.6}$$

[The formulas involving the sum-averaging over j states are the ones which are presently useful in comparison with experiment in e-N_2 scattering, because the rotational spacing has not as yet been resolved.]

We now come to the fundamental statement of the hybrid-theory: replace the abiabatic-nuclei matrix elements, Equation (5.3), by the corresponding close coupling values, Equation (4.20), for whatever partial waves are necessary:

$$a_{\varrho\lambda m}(v', v) \rightarrow a^{(m)}_{v'\ell, v\lambda} \tag{5.7}$$

(An equivalent replacement can be made for T and K matrices also.) The justification for this replacement we hope is clear. The point, we wish to reemphasize is that the time delay criterion can be theoretically (and need not be experimentally) assessed. (It should be added, however, that any such criterion is always approximate in the sense that constant of proportionality is necessarily somewhat ambiguous. In addition, in the present case the $R_0 = 2.068$ curve lies slightly removed from the main portion of the wave function, $\chi_{v=0}(R)$, of the zero vibrational function of the N_2 molecule. Thus the theoretical nature of the time delay criterion must be understood within the confines of such mundane considerations.)

Coming back to the hybrid theory, note that the purely rotational aspects of even this Π_g wave are described by vector coupling coefficients which derive from the adiabatic-nuclei theory. It is this fact which has motivated us to call this a hybrid theory. One could in principle also include rotational close coupling at the same time as vibrational close coupling (cf. Discussion). Indeed Henry[30] has

attempted that in the case of e-H_2 scattering with only limited success. The point is that the adiabatic-nuclei theory is quite sufficient,[28,31,33,34] when polarization is included, to explain the experimental data whereas vibrational-rotational close coupling even in the simpler e-H_2 case poses convergence problems of a most serious nature, and it still does not include the main effects of polarization, which—in a close coupling sense—would require higher lying electronic states as well.

The adiabatic-nuclei amplitudes were calculated from the fixed-nuclei amplitudes (the eigenphases of which are those exemplified in Table 1) using N_2 vibrational functions given by Herman and Wallis.[35] The $a_{\ell_i \ell_j m}(R)$ were interpolated, and a fifteen point gaussian quadrature was used to evaluate integral (5.3). (The j dependence of the vibrational functions in Ref. 35 was surpressed by setting $j = 0$.) All of these non-Π_g amplitudes were combined with the amplitudes $a^{(m)}_{v'\ell, v\lambda}$ for the Π_g wave ($m = 1$ even parity) from the close coupling part of the calculation according the hybrid theory prescription above for the particular v and v′ given in the results below.[36]

In Figure 7 we give the integrated vibrationally elastic ($v = 0 \rightarrow v' = 0$) cross section; the experimental result of Golden[7] is shown in the inset. Of particular note aside from the substructure itself is the agreement of the magnitude of the cross section at the peaks as well as the correct relative size of the first two peaks. The remaining peaks are not fully developed and as we have indicated this is caused primarily by lack of sufficient ℓ and v coupling due to

limitations of machine size. Although the higher peaks are also small in this experiment, they do show up more prominently in other experimental results below. The theoretical curve does not give any structure below the first peak at 1.9eV. Ehrhardt and Willmann[11] have found smooth behaviour here also, so that the older experimental structure below 1.8eV would appear to be spurious. The major discrepancy with the experiment which is not likely to be altered by further coupling is the depth of the calculated cross section between the first two peaks. Whether this could be an artifact of the measurement due to lack of sufficient energy resolution we cannot say.

We next turn to differential cross sections involving vibrationally elastic scattering. This is the first case we encounter cross term effects in the hybrid-theory between resonant (calculated with close coupling) and non resonant (calculated by adiabatic-nuclei theory) partial waves. That both cross term and quadratic effects are important can be seen by comparing Figure 8 with Figure 9. Figure 8 gives the completely calculated differential cross sections including non-resonant waves for three of the energies measured by Ehrhardt and Willmann[11] (which results are given in the inset). In Figure 9 similar results including only the Π_g partial wave are given. Not only are the latter spuriously symmetric about 90°, but the rise around 90° is completely absent both from the experiment and the full calculation. In Figure 10 the full calculation is given for the remaining three measured energies.

(given in the inset). Note again that the calculation gives absolute values, but only the relative values are measured.[11] The shapes appear in satisfactory accord with experiment.[11]

The last comparison we shall give for vibrationally elastic scattering is the differential cross section as a function of the energy at various angles (Fig. 11). We consider the comparison very satisfactory but the absence of the higher wiggles particularly in the forward directions (due to the lack of sufficient coupling in the calculation as explained above) is somewhat more apparent than in the integral cross section (Fig. 7).

We turn next to the inelastic cross sections. In Figures 12 and 13 we give the differential values at $\theta' = 20°$, $72°$ vs. k^2 respectively, these being the measurements in Reference 11 and Reference 6 respectively. In particular Schulz[6] inferred that his measurements would reflect the integrated cross sections as well. That this is so is shown in Figure 14 where the integrated cross sections are given and are seen virtually indishinguishable from the 72° curve in shape. On the other hand the absolute values which were originally inferred by Schulz[6] on the basis of summed total cross sections measured by Haas[37] are about a factor two smaller than we calculate. Thus the need for direct absolute measurements is clear, not only to test the theory but for many atmospheric applications, of which Reference 1 is one, as well. Although the shape for the inelastic $v = 0 \rightarrow v' = 1$ cross section is satisfactory, the detailed agreement

rapidly degenerates for higher v', and again this can be attributed to inadequate v and ℓ coupling as noted in going from Figure 4 to Figure 6. We believe however that the average magnitudes of the particular cross sections are meaningful for practical applications.

It should be noted that because of the virtual independence of the nonresonant amplitudes on R, essentially all of the inelastic cross sections comes from the resonant Π_g wave. This can be clearly seen in the inelastic-differential cross sections, given in Figure 15, which are quite symmetric about 90°. Although the measurements of Ehrhardt and Willmann[11] are not done over sufficiently wide angular range to prove the symmetry, the agreement with calculation in terms of ratios of forward to minimum to 90° values at the different energies is very good.

Finally we give the momentum transfer cross section. The formula for this cross section

$$\sigma_M \equiv \int \frac{d\sigma}{d\Omega'} (1 - \cos\theta') \, d\Omega' \tag{5.8a}$$

is readily integrated from (5.4) to give

$$\sigma_M = \frac{\pi}{R^2} \sum_{v'} \left[A_o(o, v') - \frac{1}{3} A_1(o, v') \right] \tag{5.8b}$$

where the $A(o, v')$ are given in (5.4b) with the Π_g amplitudes replaced again by the close-coupling amplitudes according the prescription (5.7) of the hybrid theory. (Note the $A_1(o, v') = 0$ for $v' > 0$ for Π_g). The result of the calculation is compared

with the experiment in Figure 16. The experiment as is well known does not measure σ_M directly, but rather infers it by optimizing assumed momentum transfer cross sections to fit swarm data as function of applied electric field. As such the absence of substructure on the "experimental" result should not be interpreted as its absence in fact. (It is virtually certain that the substructure must be present.) The experimental curve is seen to envelope the calculated curve in the resonance region as would be expected. About 25% of the calculated curve comes from the $v' > 0$ terms in (5.8b). However the contribution of the resonances does not extend beyond about 4 eV, thus the 20% difference in this energy range would appear at this point to remain unexplained.

Finally it is clear from (5.2) and (5.7) that the hybrid theory can be used to calculate simultaneous rotation-vibration excitation. We shall not do that here as the programming of the formulae is somewhat more ardnous, and there are presently no experiments with which to compare. (We do intend to perform that calculation at a later time.)

VI. DISCUSSION

This then completes our hybridization of vibrational close coupling and adiabatic-nuclei rotational approximations. In order to complete the a-priori theoretical framework for calculation of very narrow (probably Feshbach) resonanances, one will have to include rotational coupling as well. In that case the hybridization will take place as the second level only: i.e., the rotational

and vibrational close-coupling amplitudes for the resonant partial will be merged with the adiabatic-nuclei amplitudes for the non-resonant partial wave. We expect to elucidate the formal aspects of this generalization shortly.

Calculations involving this generalized hybrid theory will certainly be arduous. It may well be that for practical purposes other techniques (R-matrix, Fredholm determinant, etc.) may be more useful. But to be reliably accurate they will have to include the equivalent physics of the hybrid theory.

The frame-transformation theory[39,40] represents a different mix of the above theories. There one ties interior fixed-nuclei calculations to exterior close-coupling calculations at a boundary point r_0 utilizing appropriate simplifications for each region. The approach has undoubted utility in molecular photoionization and electron-molecular ion scattering where the known asymptotic Coulomb solutions can be combined with multi-channel quantum defect theory[41] to render the resonant structure to be described in terms of a few experimental parameters.[39] It should be noted, however, that even here the fixed- and adiabatic-nuclei theories can describe the non-resonant structure very well.[15,16,42]

In the case of scattering from hetero-nuclear molecules (i.e., those with a dipole moment) frame-transformation can be expected to be useful[43] if for no other reason than rendering certain cross section finite which would diverge in the fixed- and adiabatic-nuclei approximations.[44] However in the case of homonuclear diatomic molecules the utility of frame transformation is more uncertain, because the forces are probably not long-range enough to allow cross section to emerge which are suitably insensitive to the matching radius r_0.

ACKNOWLEDGMENTS

We are most grateful to Mr. Edward Sullivan for programming the adiabatic-nuclei part of this calculation. Assistance in the early stages of this investigation by Dr. Louis Wynberg is appreciated.

REFERENCES

1. G. P. Newton, J. C. G. Walker, P. H. E. Meijer, J. Geophys Research 79, 3807 (1974). G. P. Newton and J. C. G. Walker, J. Geophys Research (to be published).

2. For a review of the experimental results cf. G. J. Schulz, Rev. Mod. Phys. 45, 423 (1973).

3. Cf. Molecules in the Galactic Environment edited by M. A. Gordon and L. E. Snyder (John Wiley & Sons, New York, 1973).

4. For a review of the fixed- and adiabatic-nuclei theories (plus other theory and experiment) cf. D. E. Golden, N. F. Lane, A. Tenkin, E. Gerguoy, Rev. Mod Phys. 43, 642 (1971).

5. P. G. Burke and N. Chandra, J. Phys. B 5, 1696 (1972).

6. G. J. Schulz, Phys. Rev. 125, 229 (1962); 135, A988 (1964).

7. D. E. Golden, Phys. Rev. Lett. 17, 847 (1966).

8. A. Herzenberg and F. Mandl, Proc. Roy Soc. (London) A270, 48 (1962). For a review of the Kapur-Pierls and Siegert formalisms, which is the basis of the work of this group, cf. J. N. Bardsly and F. Mandl, Repts. Progr. of Phys. 31, 471 (1968).

9. J. C-Y. Chen, J. Chem. Phys. 40, 3507, 3513 (1964), 45, 2710 (1966); Phys. Rev. 146, 61 (1966).

10. D. T. Birtwistle and A. Herzenberg, J. Phys. B, 4, 53 (1971).

11. H. Ehrhardt and K. Willmann, Z. Physik. 204, 462 (1967).

12. M. Krauss and F. H. Mies, Phys. Rev A1, 1592 (1970).

13. F. R. Gilmore, J. Quant. Spectry. Radiative Transfer 5, 369 (1965).

14. P. G. Burke and A. L. Sinfailam, J. Phys. B 3, 641 (1970).

15. A. Temkin and K. V. Vasavada, Phys. Rev. 160, 109 (1967).

16. A. Temkin, K. V. Vasavada, E. S. Chang and A. Selvin, 186, 57 (1969).

17. R. K. Nesbet, J. Chem. Phys. 40, 3619 (1964).

18. F. H. M. Faisal and A. L. Tench, Comp. Phys. Comm. 2, 261 (1971).

19. R. M. Sternheimer, Phys. Rev. 96, 951 (1954).

20. D. L. Truhlar, Phys. Rev. A 7, 2217 (1973).

21. Equation (2.5) of Ref. 5 contains a typographical error; the imaginary factor should be $i^{\ell'-\ell}$. This is correctly reflected in our formula (3.11).

22. N. Chandra, Comp. Phys. Comm. 5, 417 (1973).

23. A. Temkin in Fundamental Interactions in Physics, Vol. 2, edited by B. Kursunoghu and A. Perlmutter (Plenum Press, New York, 1973), pp. 298 et seq.

24. A. Herzenberg in the volume cited in Ref. 23, pp. 261, et seq., has argued against the adiabatic-nuclei theory on the basis that the substructure of the Π_g resonance has a width comparable to the vibrational spacing of N_2. The argument is correct, but it depends on observation and therefore does not suffice for the needs of a predictive calculational method.

25. Vector coupling coefficients are in the form 3-j and 6-j symbols. For definitions, notation, and formulae cf. A. R. Edmonds, Angular Momentum in Quantum Mechanics (Princeton University Press, Princeton, 1957).

26. D. M. Chase, Phys. Rev. 104, 838 (1956).

27. A. Temkin and F. H. M. Faisal, Phys. Rev. A 3, 520 (1971).

28. E. Chang and A. Temkin, Phys. Rev. Lett. 23, 399 (1969).

29. This represents the first time the adiabatic-nuclei formulae for simultaneous-rotation excitation has been given explicity in full non-diagonal form. In the diagonal approximation the formulae are given in Refs. 32 and 34.

30. R. J. W. Henry, Phys. Rev. A 2, 1349 (1970).

31. S. Hara, J. Phys. Soc. Japan 27, 1592 (1969).

32. F. H. M. Faisal and A. Temkin, Phys. Rev. Lett. 28, 203 (1972).

33. R. J. W. Henry and E. S. Chang, Phys. Rev. A 5, 276 (1972).

34. A. Temkin and E. Sullivan, Phys. Rev. Lett. 33, 1057 (1974).

35. R. Herman and R. F. Wallace, J. Chem. Phys. 23, 637 (1955).

36. Results for transitions to yet higher v' states from several $v \geqslant 0$ states, needed for example in SAR problem, Refs. 1, will be compiled by the authors in the form of a NASA Technical Note.

37. R. Haas, Z. Physik 148, 177 (1957). A transmission experiment for inelastic vibrational excitation was also carried out by J. B. Hasted and A. M. Awan, J. Phys. B 2, 367 (1969) with results similar to those of Schulz, Ref. 6.

38. A. M. Englehardt, A. V. Phelps, C. G. Risk, Phys. Rev. 135, A1566 (1964).

39. U. Fano, Comments on At. and Mol. Phys. 2, 47 (1970); Phys. Rev. A 2, 353 (1970).

40. E. S. Chang and U. Fano, Phys. Rev. A 6, 173 (1972).

41. M. J. Seaton, Proc. Phys. Soc. (London) 88, 801 (1966).

42. E. S. Chang and A. Temkin, J. Phys. Soc. Japan 29, 172 (1970).

43. N. Chandra and F. A. Gianturco, Chem. Phys. Lett. 24, 326 (1974).

44. W. R. Garrett, Molec. Phys. 24, 465 (1972).

Table I

Nonresonant Eigenphase Sums as a Function of R (mod π)

Energy (eV)	Partial Wave*	Internuclear Separation R (in units of a_0)				
		1.744393	1.868	2.068	2.268	2.391607
0.20	A	-0.1921	-0.1906	-0.1985	-0.1902	-0.1926
	B	-0.0253	-0.0645	-0.0037	0.0011	0.0038
	C	0.0351	0.0295	0.0288	0.0278	0.0271
0.40	A	-0.2960	-0.2938	-0.3048	-0.2940	-0.2972
	B	-0.0366	-0.0113	-0.0090	-0.0020	0.0012
	C	0.0503	0.0423	0.0406	0.0390	0.0379
0.60	A	-0.3772	-0.3747	-0.3878	-0.3750	-0.3787
	B	-0.0505	0.0211	-0.0202	-0.0115	-0.0083
	C	0.0572	0.0474	0.0448	0.0427	0.0411
0.80	A	-0.4450	-0.4421	-0.4570	-0.4426	-0.4467
	B	-0.0673	-0.0346	-0.0353	-0.0253	-0.0223
	C	0.0591	0.0479	0.0442	0.0414	0.0394
1.00	A	-0.5037	-0.5006	-0.5170	-0.5012	-0.5056
	B	-0.0845	-0.0503	-0.0530	-0.0419	-0.0393
	C	0.0573	0.0449	0.0401	0.0368	0.0343
1.20	A	-0.5555	-0.5524	-0.5702	-0.5530	-0.5577
	B	-0.1033	-0.0677	-0.0723	-0.0603	-0.0581
	C	0.0528	0.0394	0.0337	0.0298	0.0270
1.40	A	-0.6022	-0.5989	-0.6180	-0.5997	-0.6047
	B	-0.1229	-0.0862	-0.0927	-0.0799	-0.0782
	C	0.0466	0.0323	0.0256	0.0212	0.0181
1.60	A	-0.6446	-0.6412	-0.6616	-0.6423	-0.6475
	B	-0.1428	-0.1054	-0.1137	-0.1003	-0.0990
	C	0.0389	0.0239	0.0163	0.0114	0.0081
1.80	A	-0.6835	-0.6801	-0.7018	-0.6814	-0.6869
	B	-0.1630	-0.1250	-0.1352	-0.1211	-0.1203
	C	0.0303	0.0146	0.0062	0.0009	-0.0027
2.00	A	-0.7193	-0.7158	-0.7388	-0.7176	-0.7234
	B	-0.1833	-0.1448	-0.1568	-0.1421	-0.1417
	C	0.0210	0.0046	-0.0045	-0.0102	-0.0139
2.20	A	-0.7524	-0.7480	-0.7733	-0.7514	-0.7575
	B	-0.2035	-0.1647	-0.1784	-0.1632	-0.1632
	C	0.0113	-0.0058	-0.0155	-0.0216	-0.0255
2.40	A	-0.7833	-0.7799	-0.8056	-0.7830	-0.7896
	B	-0.2235	-0.1845	-0.1999	-0.1843	-0.1846
	C	0.0011	-0.0165	-0.0269	-0.0332	-0.0373

Table I (Continued)

Energy (eV)	Partial Wave*	Internuclear Separation R in Units of a_o)				
		1.744393	1.868	2.068	2.268	2.391607
2.60	A	-0.8122	-0.8089	-0.8359	-0.8129	-0.8198
	B	-0.2434	-0.2043	-0.2213	-0.2051	-0.2058
	C	-0.0092	-0.0274	-0.0383	-0.0450	-0.0491
2.80	A	-0.8393	-0.8361	-0.8646	-0.8409	-0.8484
	B	-0.2631	-0.2239	-0.2424	-0.2258	-0.2268
	C	-0.0197	-0.0383	-0.0498	-0.0567	-0.0609
3.00	A	-0.8649	-0.8617	-0.8917	-0.8677	-0.8756
	B	-0.2825	-0.2432	-0.2633	-0.2462	-0.2474
	C	-0.0302	-0.0493	-0.0613	-0.0684	-0.0726
3.20	A	-0.8890	-0.8860	-0.9175	-0.8929	-0.9015
	B	-0.3016	-0.2623	-0.2838	-0.2664	-0.2678
	C	-0.0408	-0.0603	-0.0727	-0.0800	-0.0841
3.40	A	-0.9119	-0.9090	-0.9418	-0.9174	-0.9265
	B	-0.3204	-0.2812	-0.3041	-0.2862	-0.2878
	C	-0.0513	-0.0712	-0.0839	-0.0914	-0.0955
3.60	A	-0.9337	-0.9307	-0.9654	-0.9408	-0.9505
	B	-0.3389	-0.2997	-0.3239	-0.3056	-0.3074
	C	-0.0617	-0.0819	-0.0950	-0.1026	-0.1067
3.80	A	-0.9544	-0.9516	-0.9880	-0.9633	-0.9737
	B	-0.3570	-0.3180	-0.3434	-0.3247	-0.3266
	C	-0.0720	-0.0925	-0.1059	-0.1136	-0.1177
4.00	A	-0.9743	-0.9716	-1.0096	-0.9850	-0.9961
	B	-0.3749	-0.3359	-0.3625	-0.3434	-0.3454
	C	-0.0821	-0.1030	-0.1167	-0.1244	-0.1284
4.50	A	-1.0203	-1.0181	-1.0605	-1.0363	-1.0491
	B	-0.4179	-0.3792	-0.4087	-0.3884	-0.3907
	C	-0.1067	-0.1283	-0.1425	-0.1502	-0.1541
5.00	A	-1.0620	-1.0605	-1.1073	-1.0838	-1.0984
	B	-0.4589	-0.4204	-0.4525	-0.4311	-0.4332
	C	-0.1302	-0.1522	-0.1669	-0.1745	-0.1779

*Rows A, B, C refer to Σ_g, Σ_u, Π_u eigenphase sums respectively.

Figure Captions

Figure 1. Fixed nuclei Π_g eigenphase sum (mod π) for different internuclear separations. Note that k^2 is relative to the ground state energy of N_2 which is itself a function R; cf. bottom curve, Fig. 2.

Figure 2. Width and position of Π_g resonance vs R. The other results are from Birtwistle and Herzenberg (Ref. 10) and Krauss and Mies (Ref. 12). The lowest curve is $E_{N_2}(R) - E_{N_2}(R_o)$.

Figure 3. Some diagonal and non-diagonal potentials of the vibrational close coupling equations vs r. The corresponding fixed-nuclei potential is indicated by open circles.

Figure 4. The Π_g contribution to the vibrationally elastic cross section σ_{oo} including two and three-partial waves for increasing number of vibrational states included in the close coupling expansion.

Figure 5. Same as Fig. 4 but for $\sigma_{0\to1}(\equiv\sigma_{10})$.

Figure 6. Same as Fig. 4 but for $\sigma_{0\to2}(\equiv\sigma_{20})$.

Figure 7. The vibrationally elastic scattering in the full hybrid theory. In the inset is the experimental results of Golden (Ref. 7). In Ref. 11 the experimental structure below 1.8 eV is not found and is considered to be spurious.

Figure 8. Full hybrid theory calculation of vibrationally elastic differential cross sections at three energies. In the inset are experimental results of Ehrhardt and Willmann (Ref. 11).

Figure 9. Π_g contribution to $d\sigma_{oo}/d\Omega$. Note the symmetry and enhancement around 90° are not present in the full calculation or the experiment; cf. Fig. 8.

Figure 10. Full hybrid theory calculation of $d\sigma_{oo}/d\Omega$ at remaining three energies measured in Ref. 11 which are given in inset.

Figure 11. $d\sigma_{oo}/d\Omega$ vs k^2 for various angles. Experimental result of Ref. 11 given in inset.

Figure 12. $d\sigma_{o\to v}/d\Omega$ at $\theta = 20^{o}$ for various excited states. Experimental results of Ref. 11 given in inset.

Figure 13. Same as Fig. 12 for $\theta = 72^{o}$. In this case the experimental result (inset) is that of Schulz, second paper of Ref. 6. The ordinate of the inset show the original inferred normalization; cf. caption of Fig. 14.

Figure 14. Total vibrational excitation curves. Note similarity of shape to $\theta = 72^{o}$ curves Fig. 13 as assumed by Schulz (Ref. 6, 1964), from which the experimental result is taken. The experimental normalization however is a factor two higher than given in Ref. 6 and constitutes a new inferred normalization (Schulz, 1975 to be published). In the latter, Schulz states that the new normalization may itself be low by a factor two, which is in accord with our results.

Figure 15. Vibrationally inelastic differential cross sections compared to experiment (Ref. 11) in inset. Note that the vertical symmetry of the inelastic cross sections around 90^{o} due to minuteness of non-Π_g contribution in these cases.

Figure 16. Momentum transfer cross section compared to the one inferred from swarm experiment by Englehardt, Phelps, and Risk (Ref. 38).

PRECEDING PAGE BLANK NOT FILMED

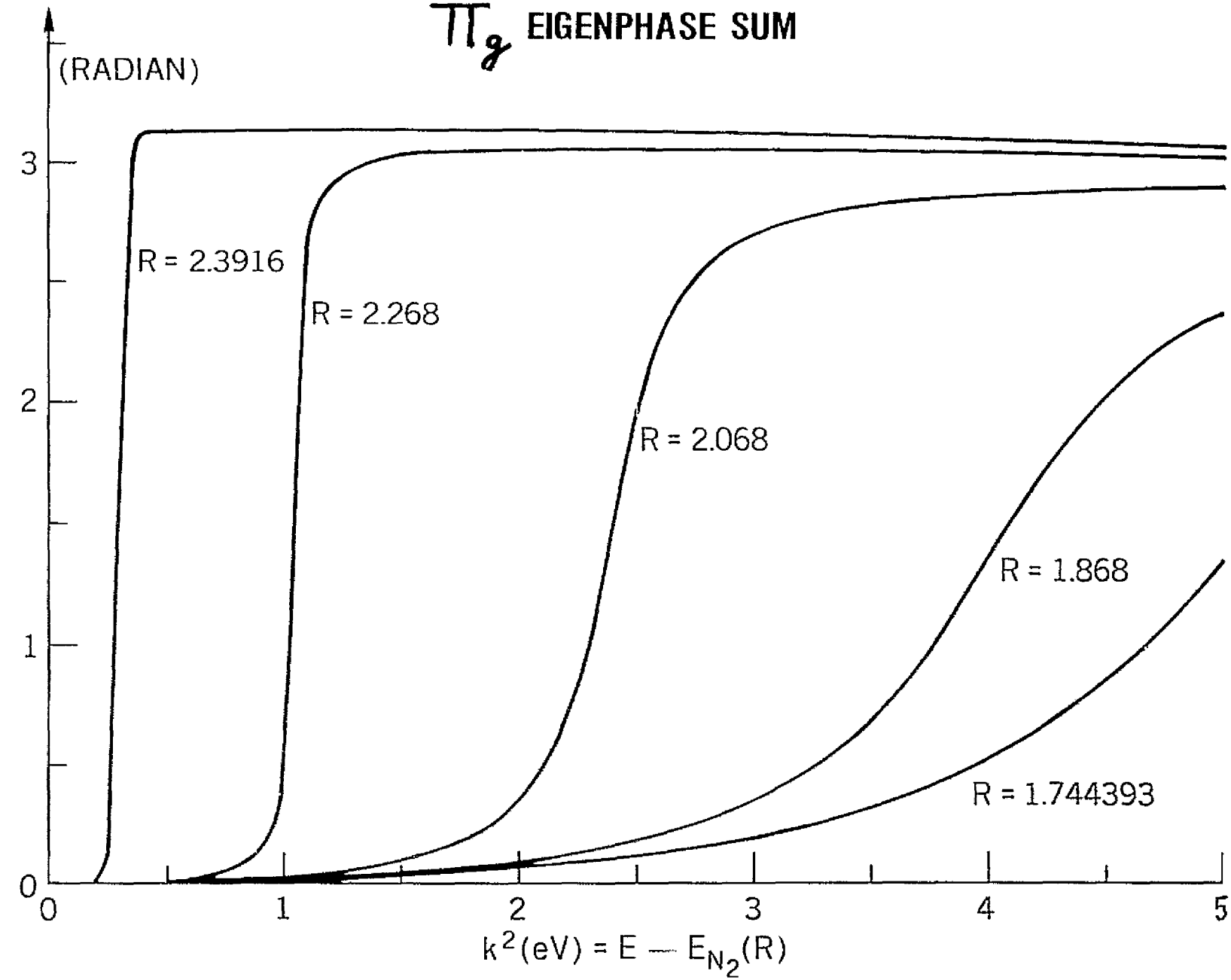

Figure 1

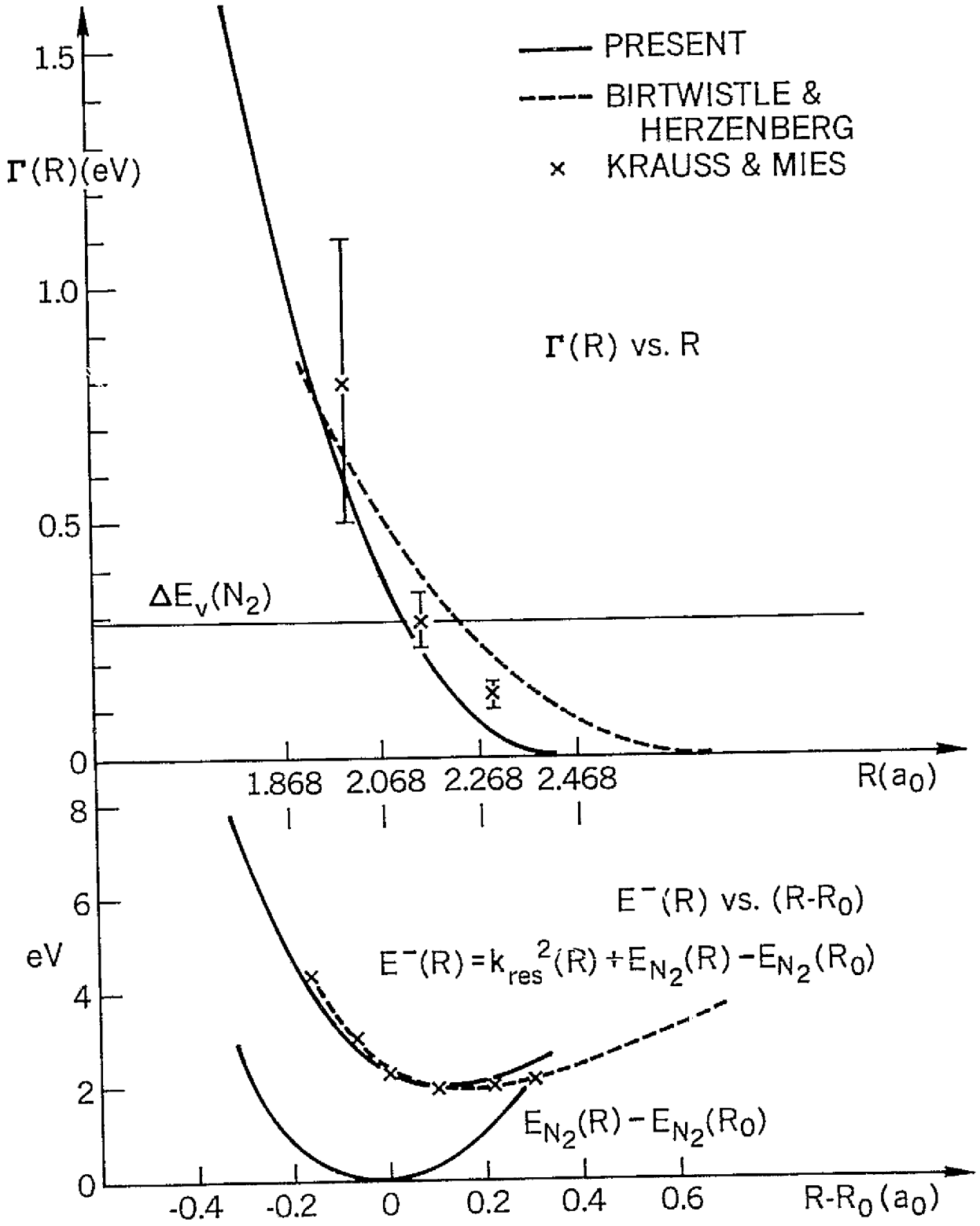
PRESENT
BIRTWISTLE & HERZENBERG
KRAUSS & MIES
Γ(R)(eV)
1.5
1.0
0.5
0
Γ(R) vs. R
ΔE_v(N_2)
1.868
2.068
2.268
2.468
R(a_0)
8
6
4
2
0
eV
E⁻(R) vs. (R-R_0)
E⁻(R) = k_res²(R) + E_N2(R) − E_N2(R_0)
E_N2(R) − E_N2(R_0)
-0.4
-0.2
0
0.2
0.4
0.6
R-R_0(a_0)

Figure 2

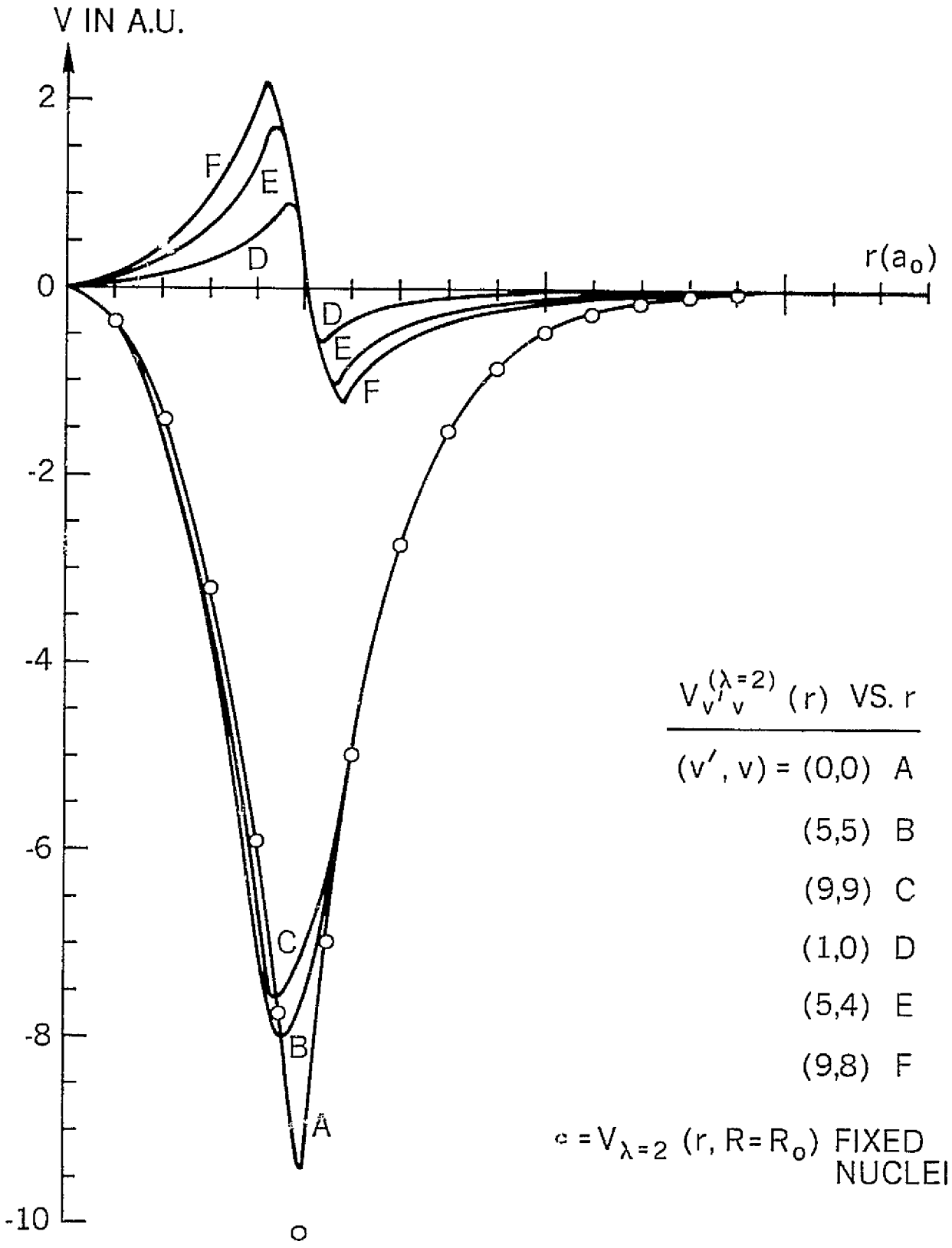
V IN A.U.
2
0
-2
-4
-6
-8
-10
r(a_o)
F
E
D
D
E
F
C
B
A
$V_{v'v}^{(\lambda=2)}(r)$ VS. r
(v', v) = (0,0) A
(5,5) B
(9,9) C
(1,0) D
(5,4) E
(9,8) F
$= V_{\lambda=2}(r, R=R_o)$ FIXED NUCLEI

Figure 3

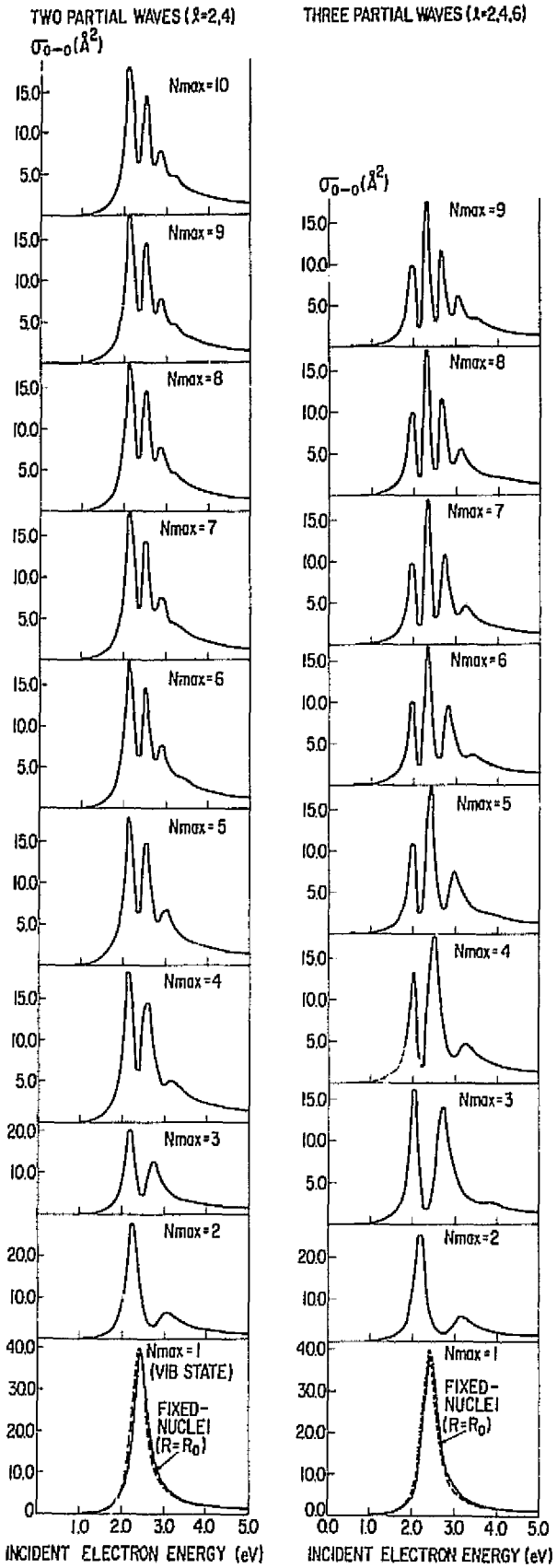
TWO PARTIAL WAVES (ℓ=2,4)
THREE PARTIAL WAVES (ℓ=2,4,6)
σ0→0(Å2)
Nmax=10
Nmax=9
Nmax=8
Nmax=7
Nmax=6
Nmax=5
Nmax=4
Nmax=3
Nmax=2
Nmax=1
(VIB STATE)
FIXED-NUCLEI (R=R0)
INCIDENT ELECTRON ENERGY (eV)

Figure 4

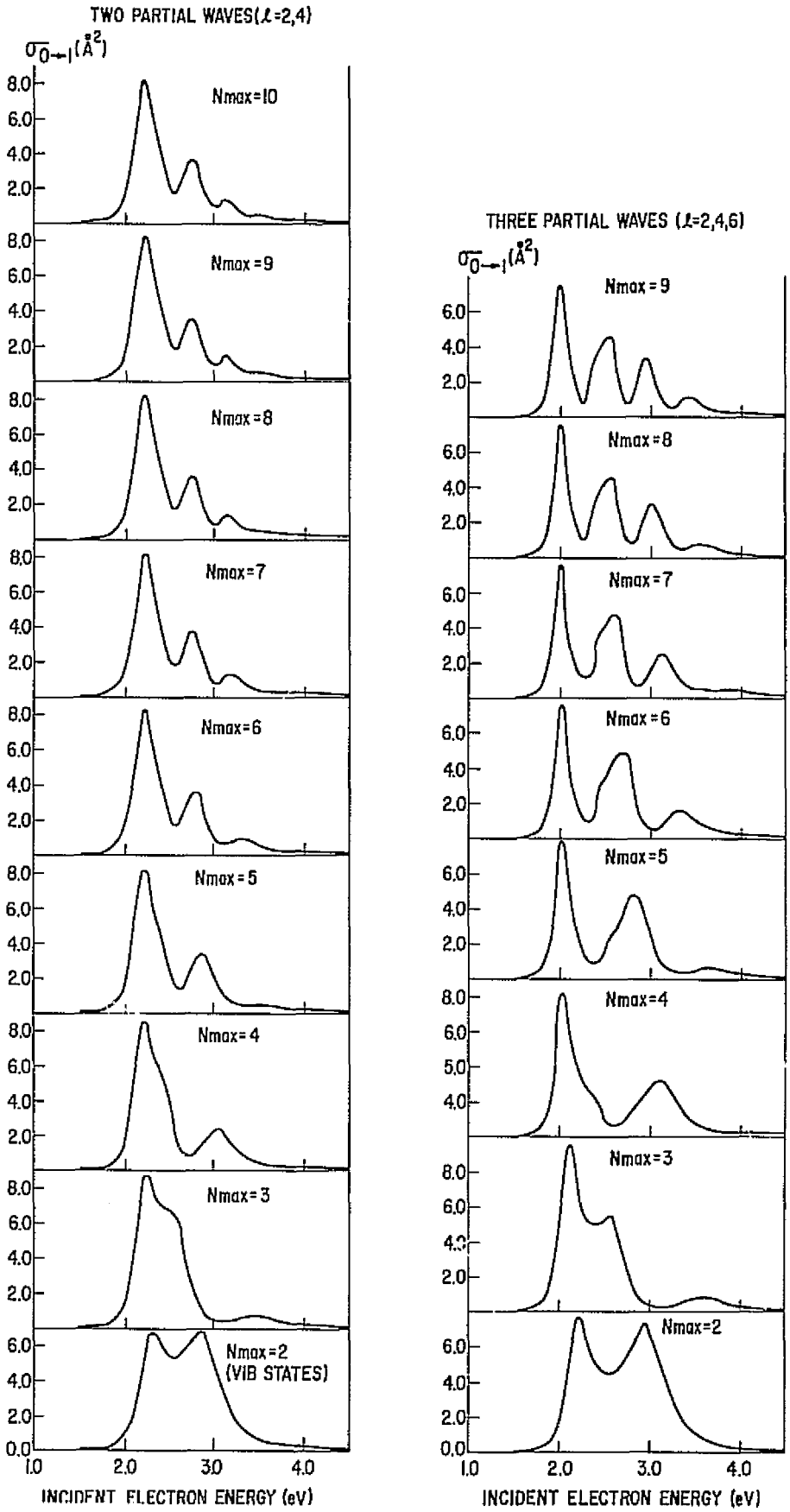
TWO PARTIAL WAVES(ℓ=2,4)
$\sigma_{0\to1}(\text{Å}^2)$
Nmax=10
Nmax=9
Nmax=8
Nmax=7
Nmax=6
Nmax=5
Nmax=4
Nmax=3
Nmax=2
(VIB STATES)
INCIDENT ELECTRON ENERGY (eV)
THREE PARTIAL WAVES (ℓ=2,4,6)
$\sigma_{0\to1}(\text{Å}^2)$
Nmax=9
Nmax=8
Nmax=7
Nmax=6
Nmax=5
Nmax=4
Nmax=3
Nmax=2
INCIDENT ELECTRON ENERGY (eV)

Figure 5

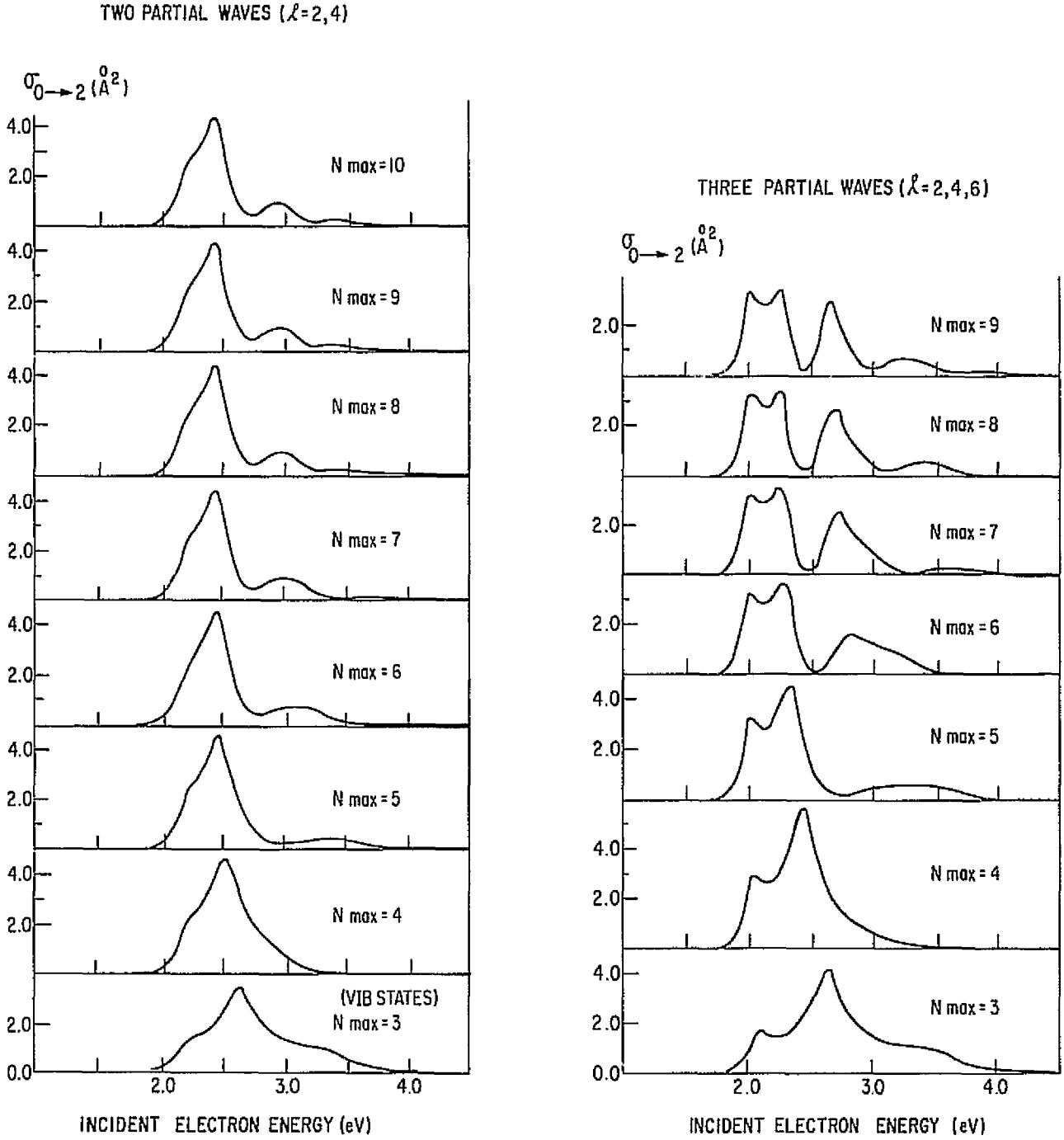
TWO PARTIAL WAVES (ℓ=2,4)
σ0→2 (Å2)
N max=10
N max=9
N max=8
N max=7
N max=6
N max=5
N max=4
(VIB STATES)
N max=3
4.0
2.0
0.0
2.0
3.0
4.0
INCIDENT ELECTRON ENERGY (eV)
THREE PARTIAL WAVES (ℓ=2,4,6)
σ0→2 (Å2)
N max=9
N max=8
N max=7
N max=6
N max=5
N max=4
N max=3
2.0
4.0
0.0
2.0
3.0
4.0
INCIDENT ELECTRON ENERGY (eV)

Figure 6

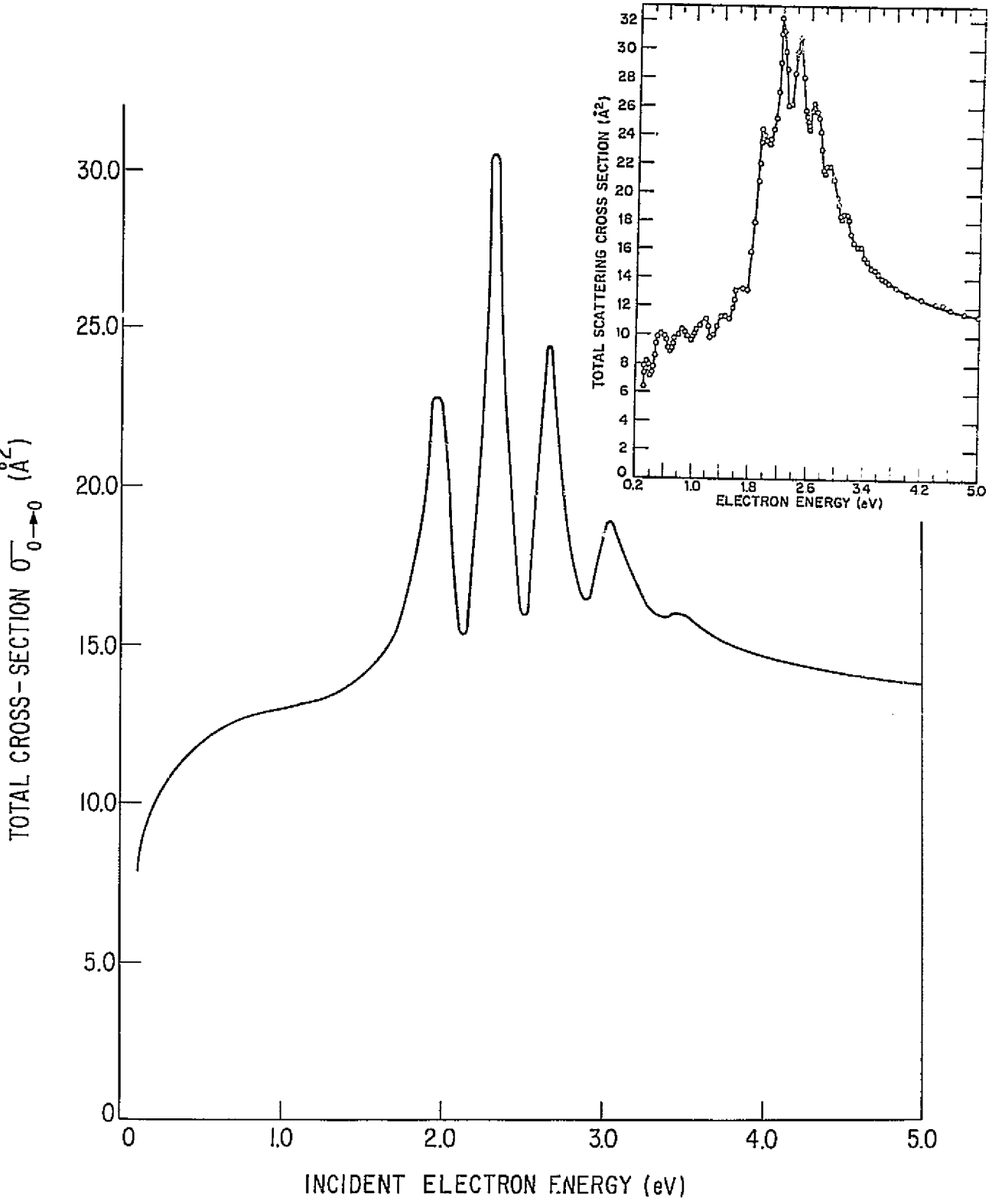
TOTAL CROSS-SECTION $\sigma_{0\to 0}$ (Å^2)
30.0
25.0
20.0
15.0
10.0
5.0
0
0
1.0
2.0
3.0
4.0
5.0
INCIDENT ELECTRON ENERGY (eV)
TOTAL SCATTERING CROSS SECTION (Å^2)
32
30
28
26
24
22
20
18
16
14
12
10
8
6
4
2
0
0.2
1.0
1.8
2.6
3.4
4.2
5.0
ELECTRON ENERGY (eV)

Figure 7

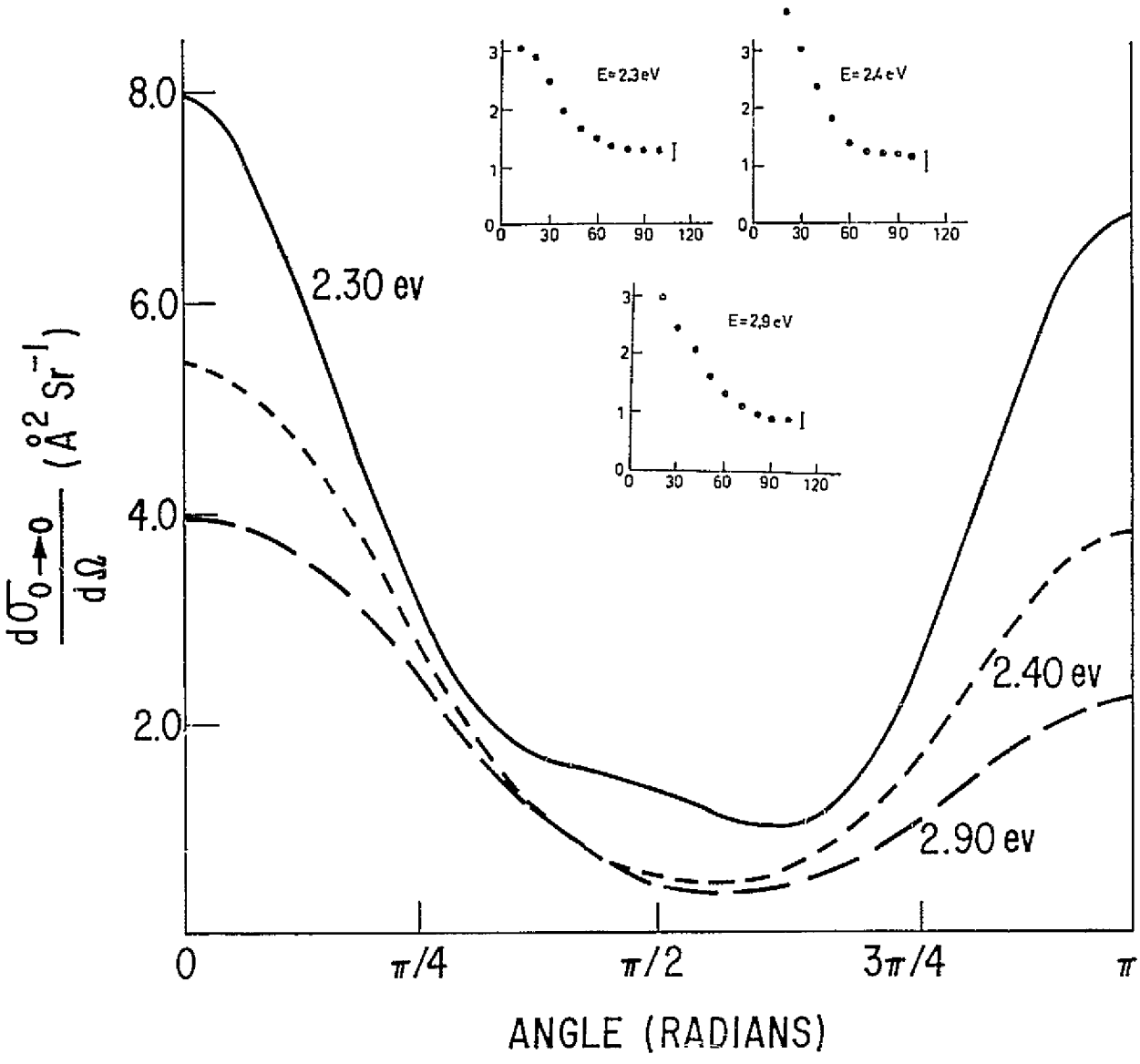
E=2.3eV
E=2.4eV
E=2.9eV
2.30 ev
2.40 ev
2.90 ev
8.0
6.0
4.0
2.0
0
π/4
π/2
3π/4
π
ANGLE (RADIANS)
dσ0→0/dΩ (Å² Sr⁻¹)

Figure 8

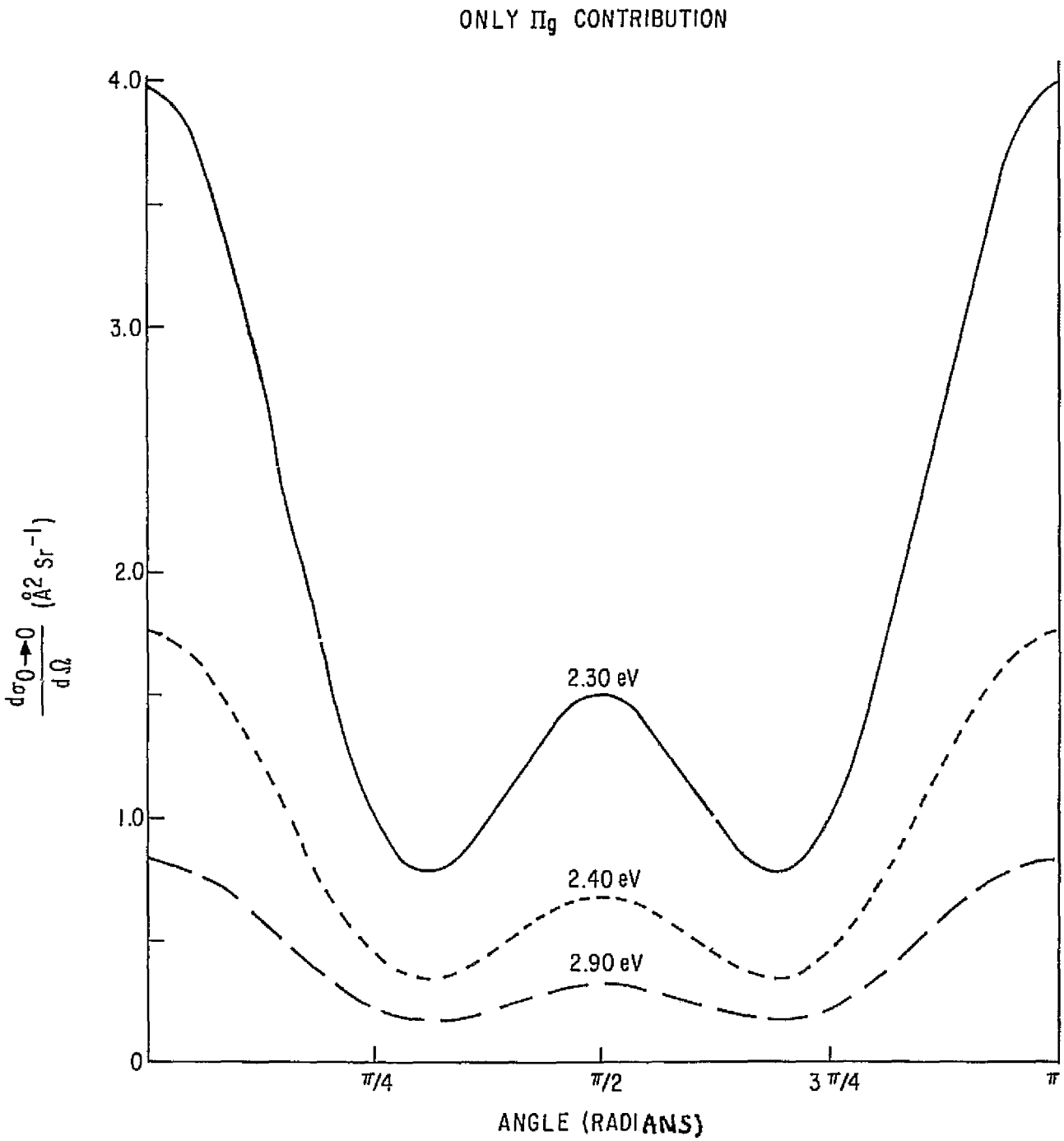
ONLY Πg CONTRIBUTION
4.0
3.0
2.0
1.0
0
2.30 eV
2.40 eV
2.90 eV
π/4
π/2
3π/4
π
ANGLE (RADIANS)
dσ0→0/dΩ (Å2 Sr-1)

Figure 9

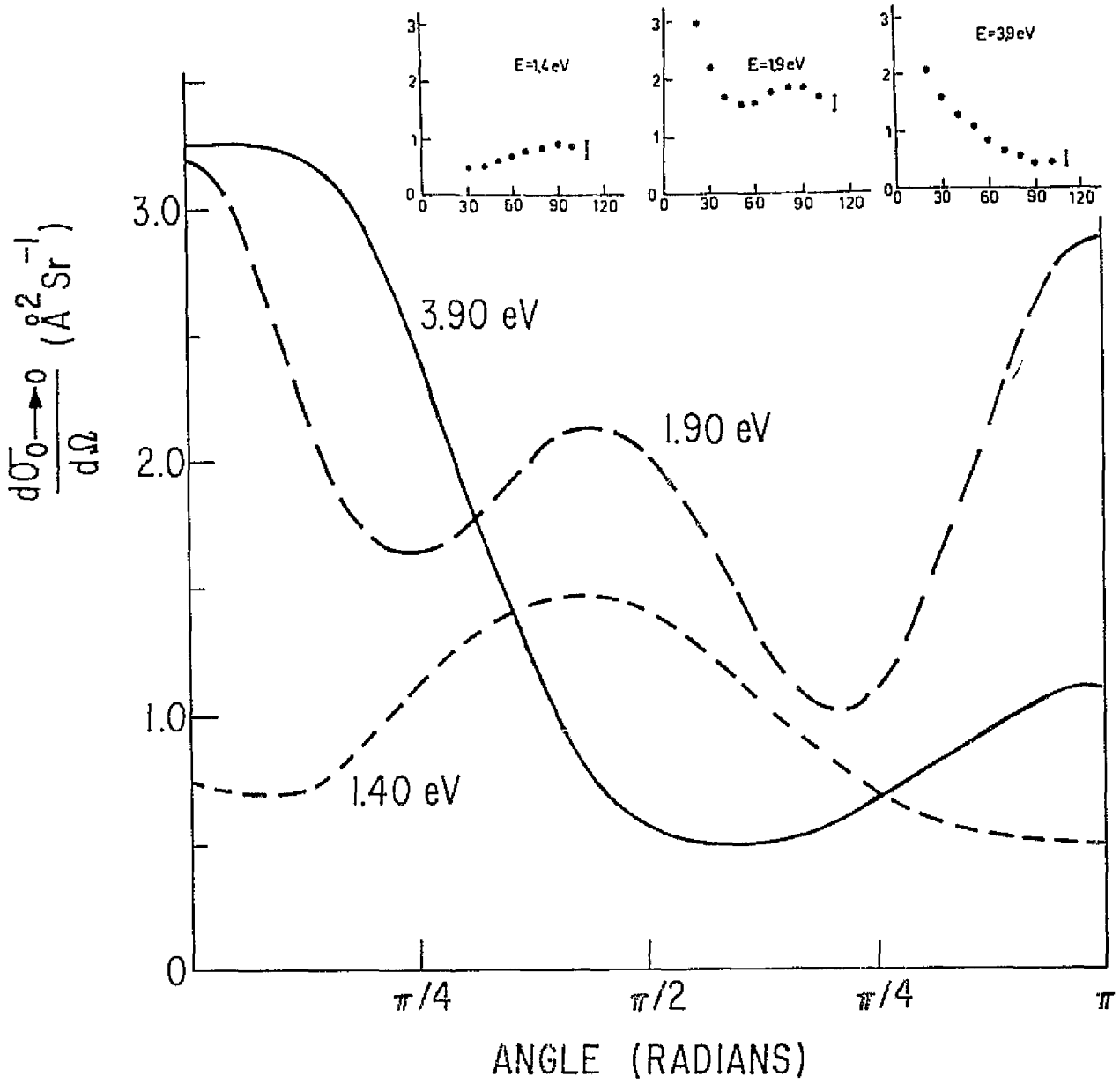
E=1.4 eV
E=1.9 eV
E=3.9 eV
3.90 eV
1.90 eV
1.40 eV
3.0
2.0
1.0
0
π/4
π/2
3π/4
π
ANGLE (RADIANS)
dσ0→0/dΩ (Å² Sr⁻¹)

Figure 10

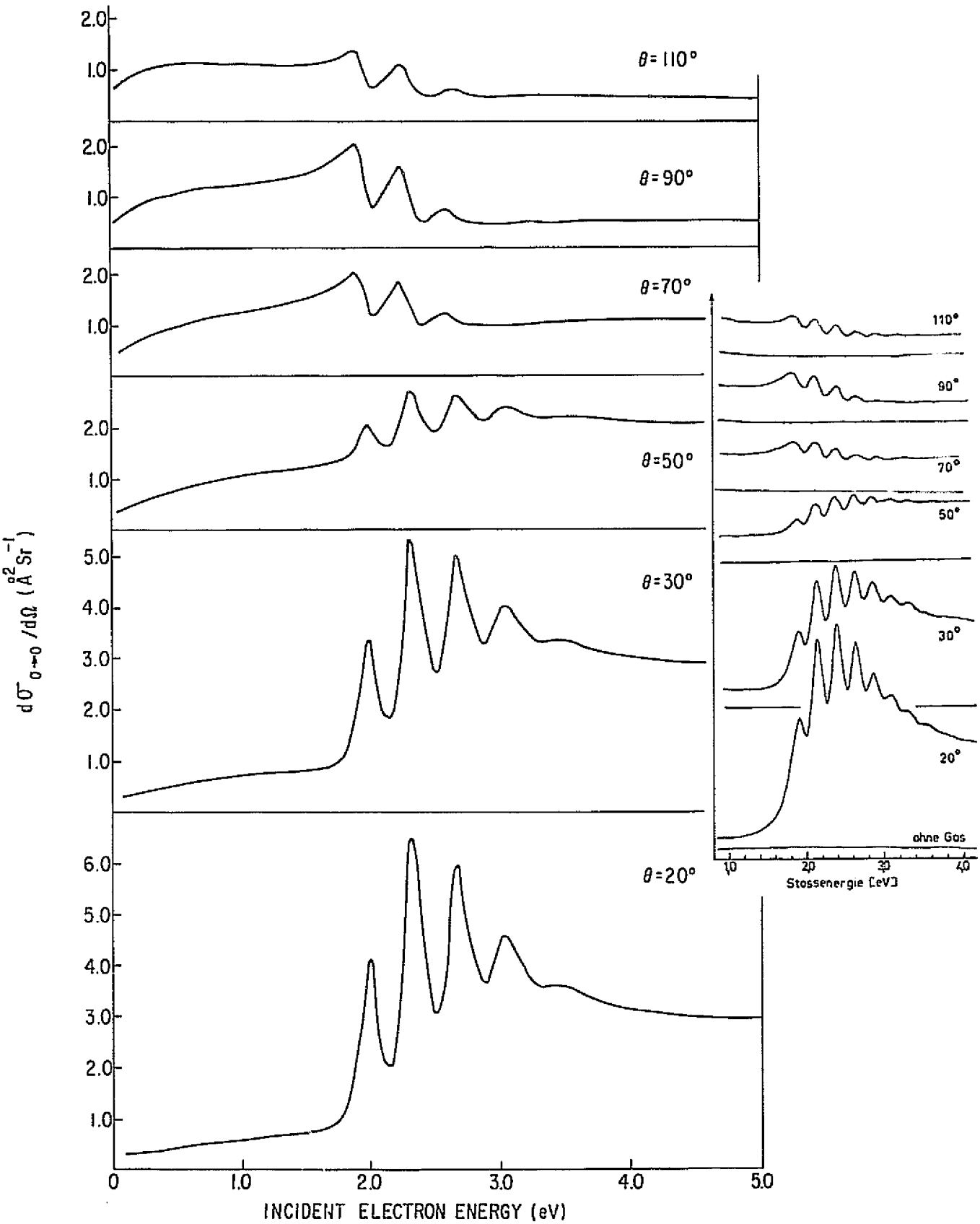
θ=110°
θ=90°
θ=70°
θ=50°
θ=30°
θ=20°
110°
90°
70°
50°
30°
20°
ohne Gas
Stossenergie [eV]
dσ 0→0 /dΩ (Å² Sr⁻¹)
INCIDENT ELECTRON ENERGY (eV)

Figure 11

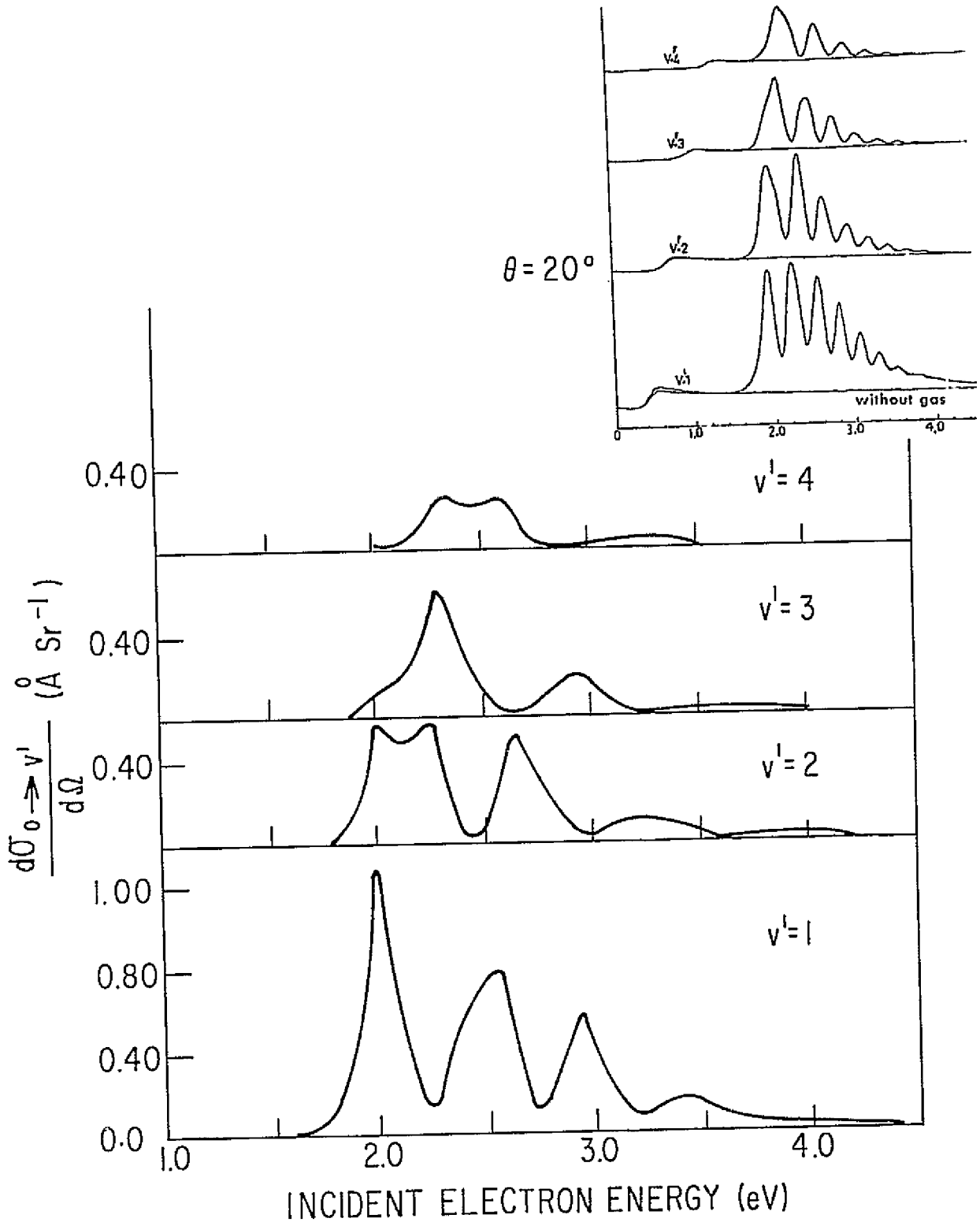
θ = 20°
v'4
v'3
v'2
v'1
without gas
0
1.0
2.0
3.0
4.0
v' = 4
v' = 3
v' = 2
v' = 1
0.40
0.40
0.40
1.00
0.80
0.40
0.0
1.0
2.0
3.0
4.0
INCIDENT ELECTRON ENERGY (eV)
dσ0→v'/dΩ (Å Sr⁻¹)

Figure 12

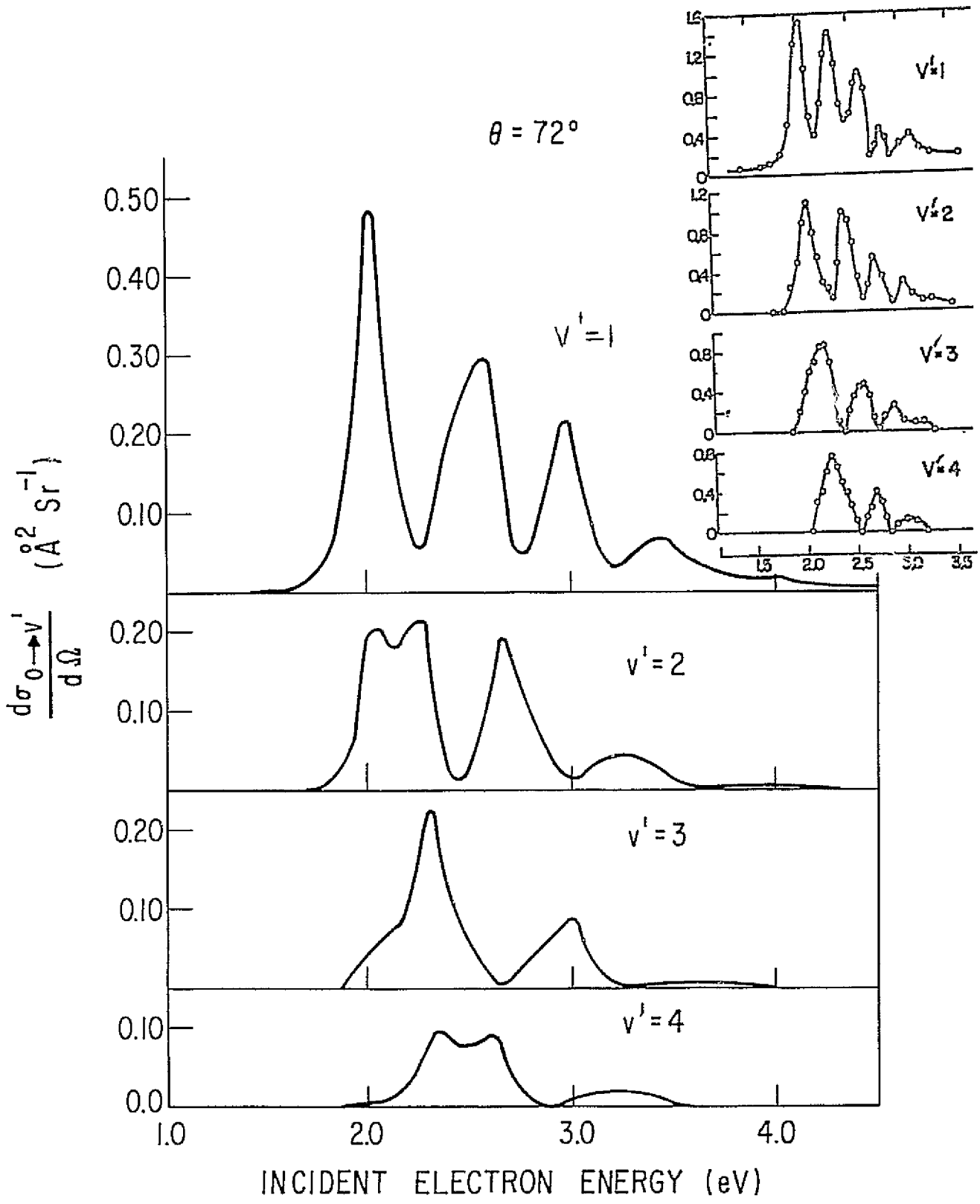
θ = 72°
v' = 1
v' = 2
v' = 3
v' = 4
0.50
0.40
0.30
0.20
0.10
0.0
1.0
2.0
3.0
4.0
INCIDENT ELECTRON ENERGY (eV)
dσ 0→v' / dΩ (Å² Sr⁻¹)
v'=1
v'=2
v'=3
v'=4
1.5
2.0
2.5
3.0
3.5

Figure 13

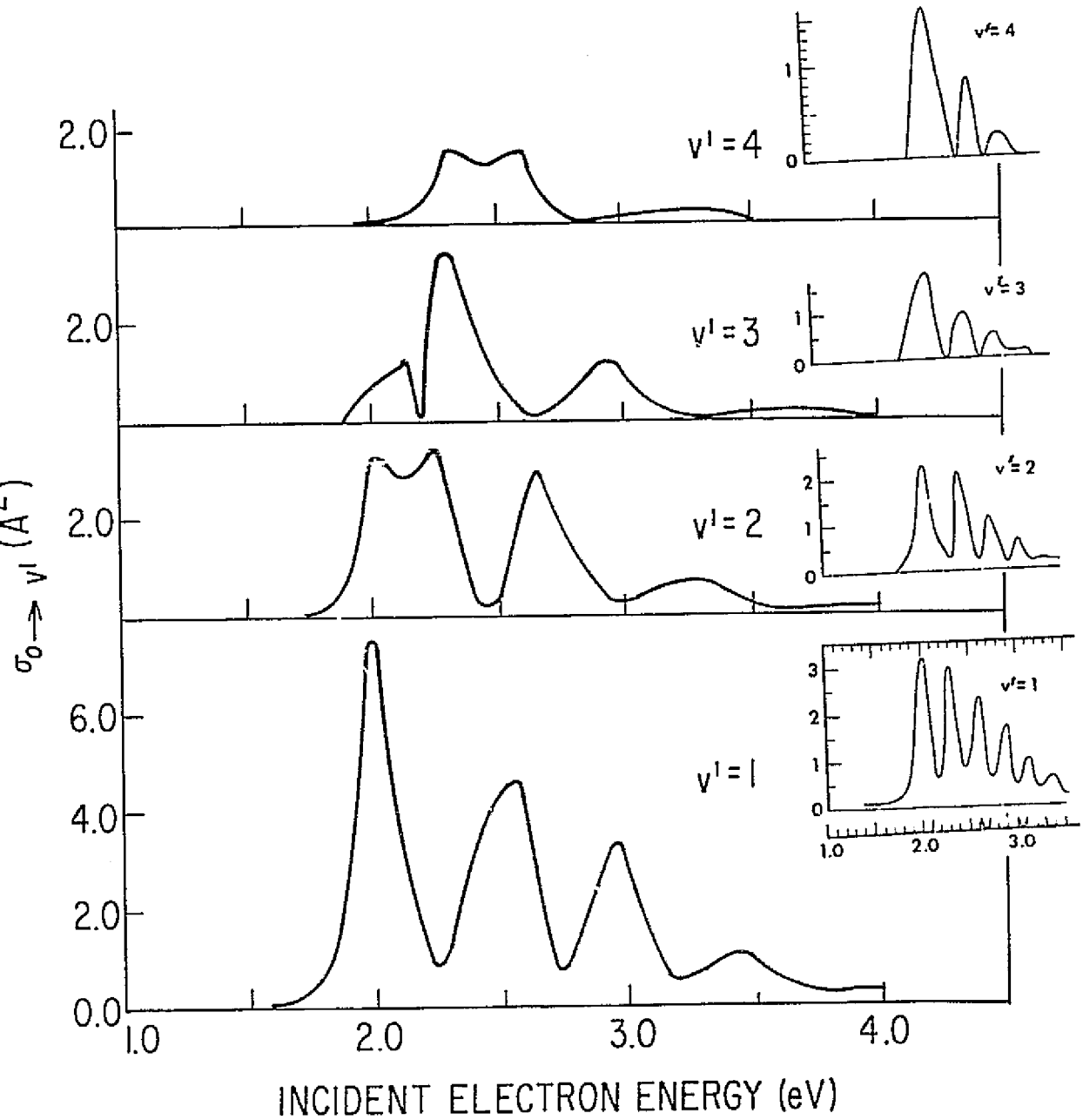
v' = 4
v' = 3
v' = 2
v' = 1
2.0
6.0
4.0
0.0
1.0
2.0
3.0
4.0
$\sigma_{0 \rightarrow v'}$ (A^2)
INCIDENT ELECTRON ENERGY (eV)

Figure 14

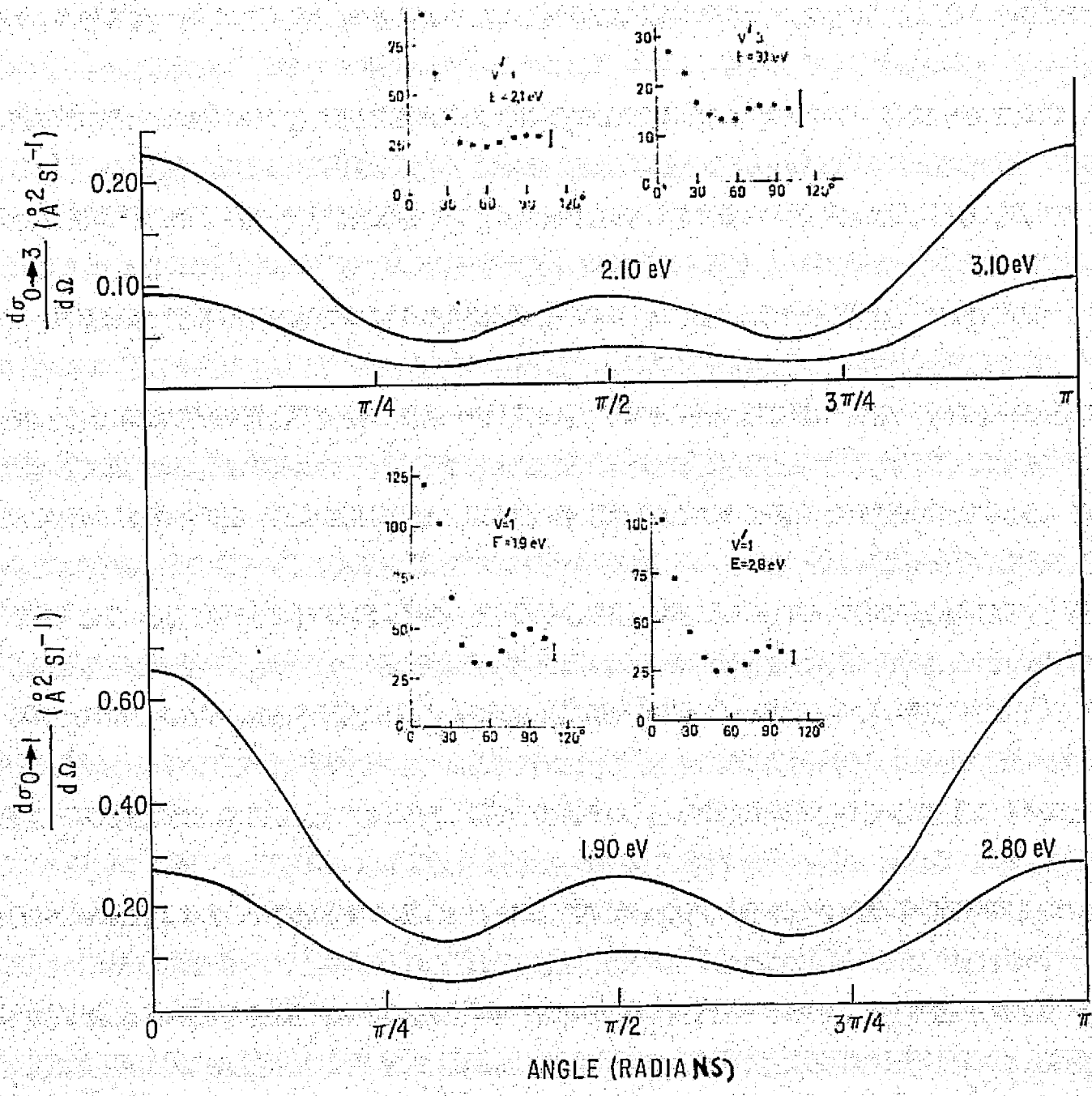
$\frac{d\sigma_{0\to3}}{d\Omega}$ ($Å^2$ sl^{-1})
0.20
0.10
2.10 eV
3.10eV
π/4
π/2
3π/4
π
$\frac{d\sigma_{0\to1}}{d\Omega}$ ($Å^2$ sl^{-1})
0.60
0.40
0.20
1.90 eV
2.80 eV
0
π/4
π/2
3π/4
π
ANGLE (RADIANS)

Figure 15

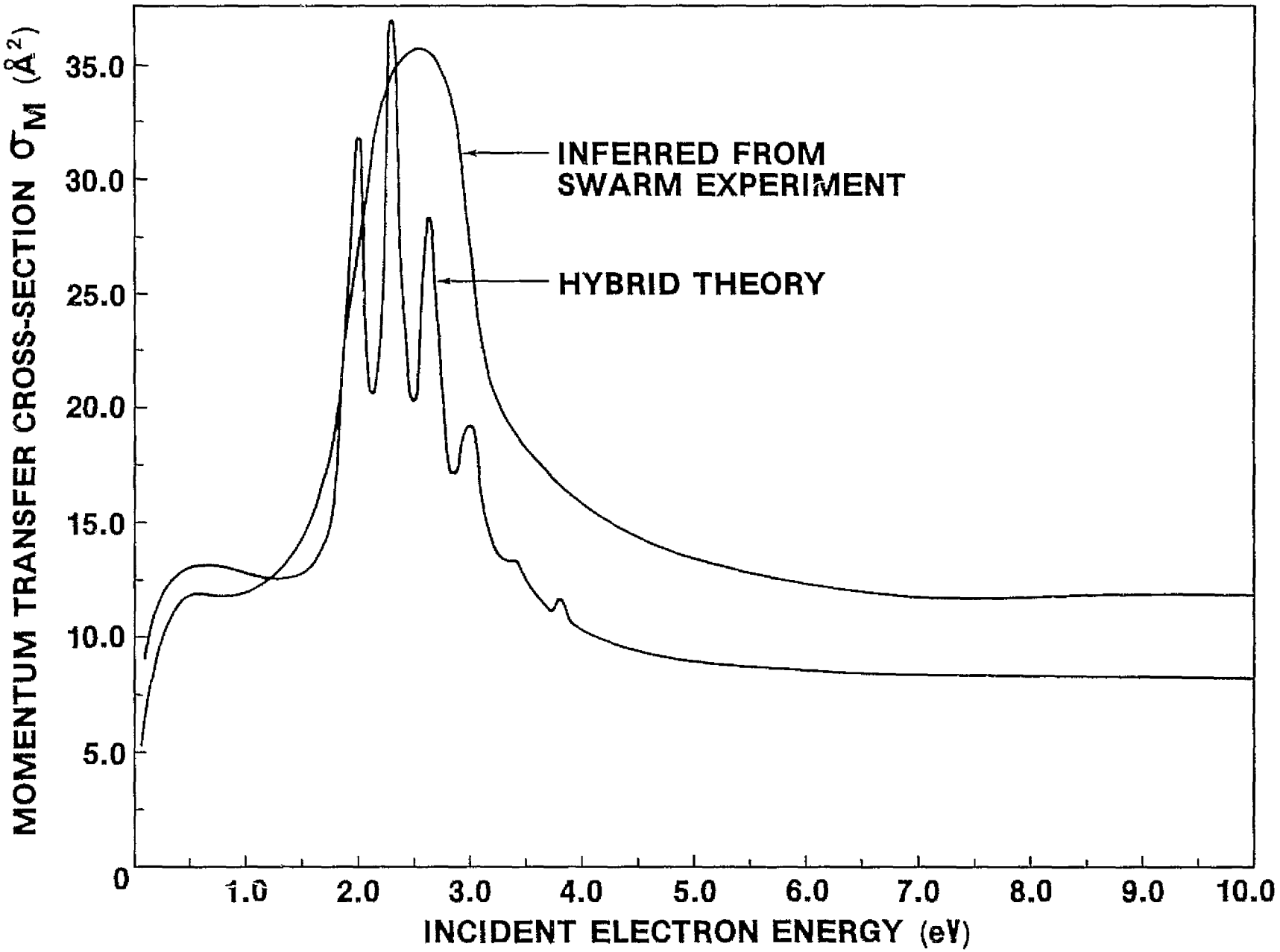
MOMENTUM TRANSFER CROSS-SECTION σ_M (Å^2)
35.0
30.0
25.0
20.0
15.0
10.0
5.0
0
INFERRED FROM
SWARM EXPERIMENT
HYBRID THEORY
1.0
2.0
3.0
4.0
5.0
6.0
7.0
8.0
9.0
10.0
INCIDENT ELECTRON ENERGY (eV)